Page 1 of 39.
doi:10.1017/aer.2020.62

An estimation method for the fuel burn and other performance characteristics of civil transport aircraft in the cruise. Part 1 fundamental quantities and governing relations for a general atmosphere

D.I.A. Poll
d.i.a.poll@cranfield.ac.uk
Emeritus Professor of Aerospace Engineering
Cranfield University
UK

U. Schumann
Deutsches Zentrum für Luft- und Raumfahrt
Institut für Physik der Atmosphäre
Oberpfaffenhofen
Germany

ABSTRACT

This paper is one of a series addressing the need for simple, yet accurate, methods for the estimation of cruise fuel burn and other important aircraft performance parameters. Here, a previously published, constant Reynolds number model for turbofan-powered, civil transport aircraft is extended to include Reynolds number effects. Provided the variation of temperature with pressure is known, the method is applicable to flight in any atmospheric conditions. For a given aircraft, cruising in a given atmosphere, there is a single Mach number and Flight Level pair, at which the fuel burn per unit distance travelled through the air has an absolute minimum value. Both these quantities depend upon the Reynolds number, which, in turn, depends upon the aircraft weight and the atmospheric vertical temperature profile. Simple, explicit expressions are developed for all parameters at the optimum condition. These are shown to be in close agreement with numerical solutions of the governing equations. It is found that typical operational mass and temperature profile variations can change cruise fuel burn rate by several percent. In the International Standard Atmosphere, when the speed and altitude deviate from their optimum values, the fuel burn penalty is reduced slightly relative

Received 4 March 2020; revised 17 June 2020; accepted 19 June 2020.

to the constant Reynolds number case. By way of example, the method is used to estimate the minimum fuel, speed-versus-height trajectory for cruise in a realistic atmosphere.

For each aircraft, cruise fuel burn is found to be governed by six independent parameters. All are constants. Two are simple, involving only size and weight, whereas four are complex and must be determined by either theoretical, or empirical, means. The estimation of these quantities will be considered in Part 2.

Keywords: fuel burn estimation; aircraft performance in cruise; environmental impact; turbofan aircraft; minimum fuel trajectory; optimum speed and altitude in a general atmosphere; Reynolds number effect on fuel burn; performance optimisation; off-optimum fuel burn performance

NOMENCLATURE

A	coefficient - Equations (32), (A-7) and (A-8)
AR	wing aspect ratio
a	constant in skin friction law (= 0.0269)– Equation (28)
a_∞	speed of sound $= (\gamma \Re T_\infty)^{1/2}$
B	coefficient - Equations (32), (A-7) and (A-9)
b	exponent in the skin friction law (= 0.14) - Equation (28)
C_d	airframe drag coefficient $= D/(0.5\gamma p_\infty (M_\infty)^2 S_{ref})$
Cd_c	compressibility drag coefficient – Equation (7)
Cd_o	zero-lift drag coefficient
Cd_w	wave drag coefficient – Equation (8)
C_L	lift coefficient $= L/(0.5\gamma p_\infty (M_\infty)^2 S_{ref})$
C_F	mean skin-friction coefficient
D	drag force
E	coefficient – Equation (14)
e	Oswald efficiency factor
FL	flight level
F_n	engine total net thrust
$f_{1,2,3.}$	functions
$G_{1,2,3.}$	atmospheric functions – Equations (79), (86), (90), (92), (95) and (98)
g	acceleration due to gravity (9.80665m/s^2 at sea level)
h	geopotential altitude
k_1	miscellaneous lift-dependent drag factor – Equation (12)
L	lift force
L_h	atmospheric temperature lapse rate with respect to geopotential height (K/m)
LR	non-dimensional, atmospheric temperature lapse rate with respect to Flight Level – Equation (76)
LCV	lower calorific value of fuel ($\approx 43 \times 10^6$ J/kg for kerosene)
L/D	lift-to-drag ratio
l	characteristic streamwise length $= S_{ref}^{1/2}$
M_∞	flight Mach number $= V_\infty / a_\infty$

$MTOM$	maximum permitted take-off mass
m	instantaneous total aircraft mass
m_f	instantaneous mass of fuel still on board the aircraft
$\dot{m}_f$	instantaneous fuel mass flow rate ($\mathrm{d}m_f/\mathrm{d}t$)
p	static pressure
R^{ac}	characteristic Reynolds number – Equation (3)
$\Re$	constant for air (287.05J/(kg K)) in the ideal gas law
S	distance travelled through the air
S_{ref}	reference wing area
s	wing span
T	static temperature
$\overline{T}$	normalised static temperature in the *ISA* – Equation (61)
t	time
V_∞	true air speed
Γ	atmospheric parameter– Equation (37)
γ	ratio of specific heats for air (=1.4)
Δ	coefficient - Equation (39)
ε	coefficient - Equation (51)
ζ	normalised Mach number - Equation (29)
η_o	propulsion system overall efficiency - Equation (2)
ι	atmospheric coefficient - Equation (68)
κ	coefficient - Equation (101), see also Equations (80) and (87)
Λ_w	wing sweepback angle measured at the $\frac{1}{4}$chord line
μ	dynamic viscosity
υ	coefficient - Equation (120)
ξ	normalised lift coefficient - Equation (29)
ρ	air density $= p/(\Re T)$
τ	coefficient - Equation (14)
ϕ	atmospheric parameter - Equation (29)
χ	altitude parameter - Equation (29)
$\psi_{0\text{-}7}$	aircraft dependent constants - Equations (9), (17), (18), (19), (21), (31) and (81)
ω	atmospheric exponent - Equation (66)

Superscripts

ac	whole aircraft value
FP	flat plate value
R	evaluated at a specified Reynolds number

Subscripts

B	when $(\eta_o L/D)$ has the maximum (best) value at a given Mach number
HS	high speed

ISA	in the International Standard Atmosphere
LS	low speed
LDm	when aircraft L/D has its maximum value for a given Mach number
max	maximum value
o	when $(\eta_o L/D)$ has its absolute maximum, or optimum, value
SL	at sea level
TP	at the tropopause
∞	flight, or freestream, value

1.0 INTRODUCTION

Fuel consumption in the cruise phase of flight is an important parameter in airline economics. However, it is also a central issue in the determination of aviation's impact upon the environment. In order to understand the interactions between the atmosphere and either an individual aircraft, or a fleet, it is necessary to have accurate estimation methods to account for the relevant parameters. To maximise their value, these must be based upon sound scientific principles, be easy to understand and be easy to use. Moreover, if they are to support high-quality, scientific work, they must also be transparent, open source and independently verifiable.

The aircraft of primary interest to the environmental science community are those that make the greatest collective contribution to global emissions. This group is dominated by the family of turbofan powered, transport aircraft, whose maximum speed is limited by the development of wave drag on their wings at Mach numbers in the transonic regime[1]. In a previous paper[(1)], it was demonstrated that, provided the Reynolds number is constant, estimates of the cruise fuel burn for this class of aircraft can be obtained by combining a series of near universal functions with three normalising parameters that are characteristics of the particular aircraft. These are the absolute maximum, or optimum, value of the product of the engine overall efficiency and the aircraft lift-to-drag ratio and the flight Mach number and aircraft lift coefficient at which this optimum occurs. The method is underpinned by dimensional analysis and captures all the relevant physics, albeit in approximate relations. This major simplification allows some important questions to be addressed by a direct analytic approach for the first time. One such question is the subject of this paper.

Maintaining constant Mach number and Reynolds number simultaneously in cruise implies flight at fixed speed and constant altitude. However, in normal service, an aircraft is operated at a range of initial (take-off) weights, altitudes and speeds. As the flight proceeds, the aircraft slowly loses weight as fuel is consumed, leaving speed and height as the variables with which the crew can control the fuel burn rate. Ideally, these would be adjusted to keep the fuel burn rate at the minimum possible value. This would place the aircraft on a classic "cruise-climb" trajectory, i.e. flying at fixed Mach number and maintaining a constant lift coefficient by steadily gaining height as the aircraft's weight reduces. However, in reality, the combination of speed and height is dictated by the air traffic control authority and the actual values flown may differ significantly from the optimum. Either way, when speed and altitude vary, there are

[1]Typically, aircraft in this category will have values of $M_{MO}\cos(\Lambda_w)$ greater than 0.7, where M_{MO} is the maximum permitted operating Mach number and Λ_w is the wing quarter-chord sweep angle.

always corresponding changes to the Reynolds number and these depend upon a combination of aircraft and atmospheric characteristics.

An aircraft's performance parameters are determined by its geometry, the flight speed and, when Reynolds number effects are taken into account, the aircraft mass and the distribution of atmospheric temperature in the vertical direction. A knowledge of the dependency of the rate of various engine emissions upon altitude is of particular importance in atmospheric science, especially in the context of NO_X impact and contrail formation. The more clearly the aircraft's behaviour is understood and the more accurate the estimates of the key variables become, the better the understanding of aviation's impact on the environment.

In this paper, the ideas described in Ref. 1 are extended to include Reynolds number effects. The application to particular aircraft, and the estimation of the aircraft specific parameters that characterise performance will be considered in a later paper.

2.0 BACKGROUND

In the cruise, the engine thrust is equal to airframe drag and the fuel consumption per unit distance travelled through the air is

$$\frac{dm_f}{dS} = -\frac{dm}{dS} = \frac{mg}{(\eta_o L/D)\, LCV}, \qquad \ldots (1)$$

where m_f is the instantaneous fuel mass, m is the instantaneous total mass of the aircraft, S is the distance travelled through the air, L is the lift, D is the drag, g is the acceleration due to gravity, LCV is the lower calorific value of the fuel and η_o is the overall propulsion efficiency of the engines, defined as

$$\eta_o = \frac{F_n V_\infty}{\dot{m}_f LCV} = \frac{DV_\infty}{\dot{m}_f LCV}, \qquad \ldots (2)$$

where F_n is the total net thrust and V_∞ is the true airspeed. Therefore, the characteristic that governs fuel efficiency is $(\eta_o L/D)$. This compound quantity represents the intrinsic aero-thermodynamic performance. The larger its value the smaller the amount of fuel needed to travel unit distance through the air and, for this reason, it is sometimes referred to as the "range parameter."

Application of dimensional analysis shows that, for a given atmosphere, the $(\eta_o L/D)$ of a turbofan powered aircraft depends upon the flight Mach number, M_∞, and an aircraft Reynolds number, R^{ac}, which may be defined as

$$R^{ac} = \frac{l\rho_\infty V_\infty}{\mu_\infty} = S_{ref}^{1/2}\left(\frac{\rho_\infty a_\infty}{\mu_\infty}\right) M_\infty = S_{ref}^{1/2}\left(\frac{\gamma p_\infty}{\mu_\infty a_\infty}\right) M_\infty \qquad \ldots (3)$$

Here, air is taken to be an ideal gas, l is a "typical" aircraft reference length, p_∞ is the atmospheric static pressure, ρ_∞ the density, a_∞ the local speed of sound, μ_∞ the dynamic viscosity and γ is the ratio of specific heats. In this study, l is taken be the square root of the reference wing area, S_{ref}. Therefore, in general, there will be a Mach number and Reynolds number pair, M_o and R_o^{ac}, at which $(\eta_o L/D)$ has its optimum value, $(\eta_o L/D)_o$. The Mach number, M_o, and the lift coefficient at the optimum condition, $(C_L)_o$, will depend upon R_o^{ac}. Furthermore, the relationships between $(\eta_o L/D)$, C_L and M_∞ will exhibit a Reynolds number dependence.

The traditional approach to the estimation of $(\eta_o L/D)$ is to construct a model from first principles using aerodynamic and thermodynamic theory. However, large civil transport aircraft generally cruise at speeds in the high subsonic range, where the optimum condition is determined by compressibility effects on the wings, up to and including shock-wave development. Unfortunately, there are no accurate, simple methods for the estimation of these effects on the airframe. Furthermore, as indicated in Fig. 2 of Ref. 1, the engines' overall propulsion efficiency, η_o, depends upon both the thrust level and the Mach number. This relationship is complex. Therefore, when considering $(\eta_o L/D)$, it is the net effect of airframe and engine Mach number dependence that must be modelled accurately and this is beyond the capability of most, if not all, simple methods.

Notwithstanding these issues, as demonstrated in Ref. 1, when the Reynolds number is constant, normalisation of $(\eta_o L/D)$, M_∞ and C_L with $(\eta_o L/D)_o$, M_o and $(C_L)_o$, yields distributions that are approximately independent of the aircraft type. This observation is found to be consistent with long established aerodynamic theory and the available data indicate that the normalising curves are accurate to $\pm 2\%$ over a wide range of operating conditions. This reduced model provides both the foundation and the starting point for the extension to include the effects of varying Reynolds number.

3.0 ROADMAP

In conventional texts on aircraft performance and design, e.g. Ref. 2, when performance parameters are being derived, Reynolds number dependent quantities are often taken to be constant. This usually reduces the complexity of the arguments considerably, but simplification comes at the expense of completeness and accuracy. Therefore, many of the "classical" aircraft performance relations, e.g. the Breguet Range Equation (Ref. 2, Chapter 15), are only strictly correct when the Reynolds number is constant. Nevertheless, given the simplicity and their familiarity within the aeronautics community, the "constant Reynolds number" relations are a good starting point and the objective of this analysis is to develop simple correction functions to account for the "real world" Reynolds number effects.

The analysis begins with a brief review of the governing equations and an introduction to the relevant "constant Reynolds number" relations. Terms in these relations that have viscous drag dependence are then linked to Reynolds number through a skin-friction law. These extended relations are then combined with the "universal" constant Reynolds number functions developed in Ref. 1 to find the isobar and Mach number at which $(\eta_o L/D)$ has its optimum value for an aircraft of given mass in a completely general atmosphere. The results take the form of correction factors applied to the constant Reynolds number values for $(C_L)_o$ and M_o, whilst the effect of atmospheric temperature variations is shown to be captured by a single parameter. The atmospheric parameter is then analysed, approximated and simplified by expressing the characteristics of a general atmosphere in the form of a perturbation from the familiar International Standard Atmosphere. With these elements in place, an expression for the Reynolds number at $(\eta_o L/D)_o$ is derived and this is used to obtain expressions for $(\eta_o L/D)_o$, $(C_L)_o$ and M_o that capture all Reynolds number effects and are applicable in a completely general atmosphere. Comparisons between the analytic solution and direct numerical solutions of the governing equations are used to check accuracy. Off-optimum conditions are also addressed, since moving away from the optimum necessarily involves changes in Reynolds number. Variation of Mach number at constant Flight Level and variation of Flight Level at constant Mach number, for an aircraft of fixed mass, are expected to differ from the "constant Reynolds number" curves identified in Ref. 1 and comparisons are made.

3.1 Governing equations

The variation of the drag force with lift is given by the aircraft's "drag polar." This depends upon Mach number and Reynolds number and the complete polar covers all phases of flight, including the take-off and landing. However, for the current purposes, attention is restricted to that portion of the "trimmed"[2] polar that is relevant to cruise, i.e. flight at transonic speeds. Hence, the ranges of lift coefficient and Mach number that need to be considered are greatly reduced and, consequently, it is usually possible to represent the relevant portion, accurately, with an expression of the form

$$Cd = \frac{D}{(\gamma/2)\, p_\infty M_\infty^2 S_{ref}} \approx (Cd_o)_{HS} + (Cd_i)_{HS} C_L^2 = (Cd_o)_{HS} + \left(\frac{1}{\pi .AR.e_{HS}}\right) C_L^2 \quad \ldots (4)$$

Here, C_L is the lift coefficient, defined as

$$C_L = \frac{mg}{(\gamma/2)\, p_\infty M_\infty^2 S_{ref}} \quad \ldots (5)$$

In addition, $(Cd_o)_{HS}$ is the high-speed, zero-lift drag coefficient, $(Cd_i)_{HS}$ is the high-speed, lift dependent drag coefficient, e_{HS} is the high-speed Oswald efficiency factor and AR is the wing aspect ratio, defined as

$$AR = \frac{s^2}{S_{ref}}, \quad \ldots (6)$$

where s is the wingspan.

The primary source of lift-dependent drag is the induced, or vortex, drag acting on the wings. This mechanism is described in standard aerodynamics texts, e.g. Ref. 2. However, on a complete aircraft configuration, there are other sources of vortex drag, e.g. drag due to the trimming load on the tailplane and drag due to lift generated on the fuselage. In addition, there are lift-dependent drag contributions that are not vortex related. These arise because a change in lift alters the pressure distributions over the various components. This, in turn, changes the boundary layer development and, hence, the component's profile drag. All these lift-related effects are captured by the Oswald factor.

In general, the high-speed quantities appearing in Equation (4) are Mach number dependent and difficult to estimate. However, their low-speed values can be determined with reasonable accuracy using classical aerodynamic theory. Consequently, it is convenient to recast Equation (4) in the form

$$Cd \approx Cd_0 + \left(\frac{1}{\pi .AR.e_{LS}}\right) C_L^2 + Cd_c, \quad \ldots (7)$$

where, Cd_0, and e_{LS} have their low-speed, or incompressible, values and Cd_c is the compressibility drag coefficient. Compressibility drag captures all the effects of Mach number. Initially,

[2] At every point on the trimmed drag polar, the tail load is set to the value at which the net pitching moment about the aircraft's centre of gravity is zero, as it would be in steady, straight and level flight. This introduces a small element of trim drag that depends upon the centre of gravity location.

these come from skin friction variation and changes to the surface pressure distribution, with the consequential impact upon boundary layer development and profile drag. At sufficiently high Mach numbers, the surface pressures change due to the establishment of local regions of supersonic flow. Eventually, shock waves form. These produce further modifications to the wing pressure distribution and involve complex interactions with the boundary layer. At Mach numbers below those at which regions of supersonic flow appear, Cd_c increases slowly as the Mach number increases due to the changing pressure distribution, whilst decreasing slowly due to the reducing surface friction. However, as described in Ref. 2 (Chapter 12), above a Mach number of about 0.5, these opposing effects are usually assumed to cancel each other out and Cd_0 becomes independent of Mach number. In addition, according to classical aerodynamic theory, e.g. Refs 2 and 3, below the speeds at which shock waves form, the Oswald factor is approximately independent of Mach number. Therefore, for Mach numbers greater than 0.5, Equation (7) may be written as

$$Cd \approx (Cd_0)_{M=0.5} + \left(\frac{1}{\pi .AR.e_{LS}}\right) C_L^2 + Cd_w, \qquad \ldots (8)$$

where Cd_w is now that part of the drag resulting from the development of significant regions of supersonic flow at the wing surface and, eventually, due to shock wave formation. These high Mach number effects are often referred to collectively as "wave drag", e.g. see Ref. 2, and, in general, Cd_w depends upon Mach number, lift coefficient and, to a lesser extent, Reynolds number. Since the zero-lift, profile drag coefficient is directly proportional to the mean skin-friction coefficient, it may be linked to the drag coefficient of a flat plate at zero incidence, C_F^{FP}, and a Mach number of 0.5, i.e.

$$Cd_0 \approx \psi_0 \left(C_F^{FP}\right)_{M=0.5} = \psi_0 \left(C_F^{ac}\right), \qquad \ldots (9)$$

where the constant of proportionality, ψ_0, depends only on the aircraft geometry and C_F^{ac} depends only on the aircraft's flight Reynolds number.

If the Reynolds number and, hence, C_F are constant[3], then, in the absence of wave drag ($Cd_w = 0$), Equations (8) and (9) may be combined to show that the lift-to-drag ratio ($L/D = C_L/C_d$) exhibits a maximum, whose value only depends upon the aircraft geometry, the Oswald factor and the magnitude of the mean skin-friction coefficient, i.e.

$$\left(\frac{L}{D}\right)_{max} \approx \frac{1}{2}\left(\frac{\pi .AR.e_{LS}}{\psi_0}\right)^{1/2}\left(\frac{1}{C_F^{ac}}\right)^{1/2}, \qquad \ldots (10)$$

when

$$(C_L)_{LDm} \approx (\pi .AR.e_{LS}\cdot\psi_0)^{1/2}\left(C_F^{ac}\right)^{1/2} \qquad \ldots (11)$$

As already noted, the Oswald factor contains elements of both vortex and non-vortex drag. However, it depends, primarily, upon the wing form drag. Consequently, it is expected to depend not only upon geometric parameters, but also upon the zero-lift, profile drag

[3]When the Reynolds number is constant, Cd_0 is independent of C_L.

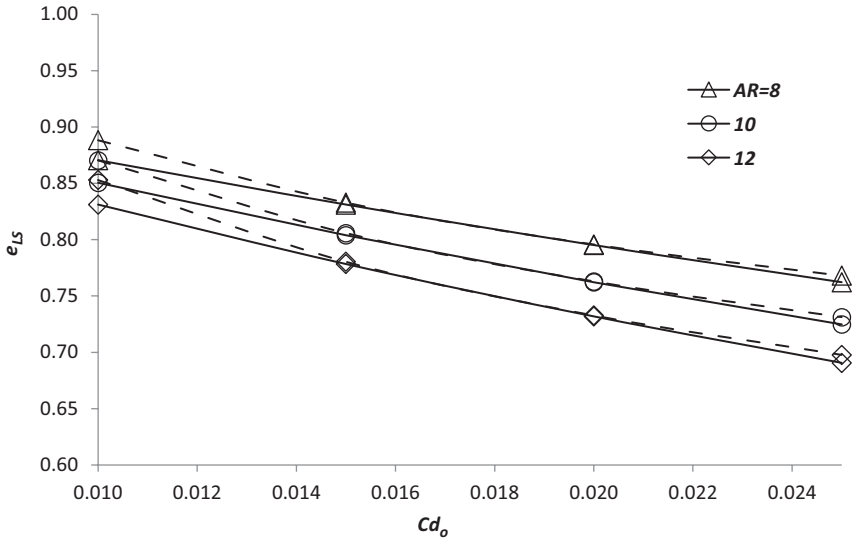

Figure 1. Examples of the variation of the low-speed, Oswald efficiency factor with the zero-lift, profile drag coefficient and aspect ratio. Full lines are Equation (12) and dashed lines are power-law approximations that are exact when Cd_o is 0.0175. The wing sweep is taken to be 30°.

coefficient, Cd_o. As described by Shevell[4] in Ref. 2 (Chapter 11, Fig. 11.8), for this class of aircraft, e_{LS} depends, primarily, upon wing aspect ratio, wing sweep angle and Cd_o. It is usually expressed in the form

$$e_{LS} \approx \frac{1}{(1.04 + (\pi .AR.k_1))} \qquad \ldots (12)$$

Here, the empirical factor 1.04 represents the vortex drag element, whilst k_1 captures the miscellaneous, lift-dependent drag effects. Shevell's data suggest that k_1 may be represented by the approximate relation

$$k_1 \approx 0.80\,(1 - 0.53cos\,(\Lambda_w))\,Cd_o, \qquad \ldots (13)$$

where Λ_w is the wing sweep angle measured at the $1/4$ chord line. Examples of this variation, based upon typical aircraft characteristics, are plotted in Fig. 1. However, given the form of Equations (10) and (11) and recognising that, in practice, the maximum changes in Cd_o due to Reynolds number variation of an aircraft in flight are only about 10%, it is convenient to replace Equation (12) with a local, power-law approximation of the form

$$e_{LS} \propto \left(\frac{1}{Cd_o}\right)^{\tau} \approx \frac{E}{\left(C_F^{ac}\right)^{\tau}} \text{ where } \tau = -\left(\frac{C_F^{ac}}{e_{LS}}\right)\frac{de_{LS}}{dC_F^{ac}}, \qquad \ldots (14)$$

[4]Richard S. Shevell was chief of the aerodynamics section at Douglas Aircraft from 1959 until 1967 and, subsequently, director of the commercial advanced design department until 1970. Although not specifically stated, it is believed that the many empirical relations given in his book are based upon data from the Douglas Aircraft, aerodynamics section.

where the coefficients E and τ are constants that depend only upon the aircraft geometry and are determined at a representative value of Cd_o. This form is also given in Fig. 1, where the power-law coefficients have been determined by matching both e_{LS} and its gradient, as determined from Equation (12), when Cd_o is 0.0175. For values of Cd_o lying in the range 0.015 (−14%) to 0.020 (+14%), the difference between Equations (12) and (14) is found to be less than 0.25%. Therefore, the power-law form is accurate enough for the current purposes. These sample calculations also indicate that, in general, τ lies in the range 0.10 to 0.25. Consequently, variations in e_{LS} resulting from changes in C_F and, hence, Reynolds number are expected to be significant.

Hence, Equations (10) and (11) become

$$\left(\frac{L}{D}\right)_{max} \approx \frac{1}{2}\left(\frac{\pi.AR.E}{\psi_0}\right)^{1/2}\left(\frac{1}{C_F^{ac}}\right)^{\left(\frac{1+\tau}{2}\right)} \quad \ldots(15)$$

and

$$(C_L)_{LDm} \approx (\pi.AR.E.\psi_0)^{1/2}\left(C_F^{ac}\right)^{\left(\frac{1-\tau}{2}\right)} \quad \ldots(16)$$

Now consider a situation in which, as the Mach number increases, the cruise altitude is increased by just enough to keep the Reynolds number and, hence, the mean skin-friction coefficient constant. When the Mach number exceeds the value at which "compressibility drag" becomes significant, the maximum (L/D) begins to drop below the level indicated in Equation (15) and continues to reduce at a rate that increases rapidly with further increases in Mach number. At the same time, the engine overall propulsive efficiency, η_o, which, as shown in Appendix B of Ref. 1, is a strong function of Mach number, is rising monotonically as M_∞ increases. Therefore, at some point in the high-subsonic speed range, $(\eta_o L/D)$ must have an absolute maximum and the Mach number at this condition is M_o.

Simple methods for the estimation of wave drag are rare in the open literature. However, one useful example is provided by Shevell in Ref. 2, where Cd_w is presented as a function of Mach number and lift coefficient. As indicated in Fig. 12.13 of Ref. 2, the variation with Mach number is such that the gradient $\mathrm{d}Cd_w/\mathrm{d}M_\infty$ increases very rapidly as Mach number increases and the embedded shock waves become stronger. However, Cd_w itself stays relatively small, having maximum values in the region of 0.0020 ($\approx$ 10% of Cd_o).

This being the case, as Mach number increases, the values of $(L/D)_{max}$ and the lift coefficient at which the maximum L/D occurs, whilst reducing, still remain quite close to the values given in Equations (15) and (16). An example showing this general behaviour is provided in Fig. 15.16 of Ref. 2. The deviations from the low-speed values are due, primarily, to the Mach number dependence of the wave drag. Furthermore, as demonstrated in Appendix B of Ref. 1 and also discussed in detail by Cumpsty and Hayes in Chapter 8 of Ref. 4, application of dimensional analysis to the overall engine flow shows that, whilst η_o depends on M_∞ and, to a lesser extent, on the net thrust being produced, it is independent of R^{ac}. Therefore, at the optimum condition, both M_o and η_o are essentially independent of R^{ac}. It follows that, when the Reynolds number is constant everywhere, the predominant dependencies at the optimum condition are

$$(\eta_o L/D)_o^R \approx \psi_1\left(\frac{1}{C_F^{ac}}\right)^{\left(\frac{1+\tau}{2}\right)}, \quad \ldots(17)$$

$$(C_L)_o^R \approx \psi_2 \left(C_F^{ac}\right)^{\left(\frac{1-\tau}{2}\right)}, \quad \ldots (18)$$

$$\left(\frac{L}{D}\right)_o^R \approx \psi_3 \left(\frac{1}{C_F^{ac}}\right)^{\left(\frac{1+\tau}{2}\right)} \quad \ldots (19)$$

and

$$M_o^R \approx \psi_4, \quad \ldots (20)$$

where, from Equation (14),

$$\tau = -\left(\frac{C_F^{ac}}{e_o}\right)\frac{de_o}{dC_F^{ac}} \quad \ldots (21)$$

and the superscript R indicates that the quantity is evaluated at a particular value of R^{ac}. It is also important to note that ψ_0, ψ_1,ψ_2, ψ_3 andψ_4 are constant and characteristics of the aircraft and engine combination.

In Ref. 1, it is shown that, for a given Reynolds number, when the variations of $(\eta_o L/D)$ with cruise Mach number and lift coefficient are normalised with $(\eta_o L/D)_o$, M_o and $(C_L)_o$, the resulting distributions are approximately independent of the aircraft type. These universal functions are listed in Appendix A and the result may be summarised in the statement

$$\frac{(\eta_o L/D)}{(\eta_o L/D)_o^R} = function\left(\frac{C_L}{(C_L)_o^R}, \frac{M_\infty}{M_o^R}\right) \quad \ldots (22)$$

That is to say, at a given Reynolds number, $(\eta_o L/D)$ is a function of the independent variables C_L and M_∞ and the values of three, aircraft specific, parameters at the optimum condition, i.e. $(C_L)_o^R$, M_o^R, and $(\eta_o L/D)_o^R$. This result can be extended to include Reynolds number variation by retaining the same functional relationships, but with the constants $(\eta_o L/D)_o^R$, $(C_L)_o^R$ and M_o^R being replaced by the functions given in Equations (17), (18) and (20), i.e.

$$\frac{(\eta_o L/D)}{\psi_1}\left(C_F^{ac}\right)^{\left(\frac{1+\tau}{2}\right)} = function\left(\frac{C_L}{\psi_2}\left(\frac{1}{C_F^{ac}}\right)^{\left(\frac{1-\tau}{2}\right)}, \frac{M_\infty}{\psi_4}\right). \quad \ldots (23)$$

The equation set is closed by specifying the relationship between the flat-plate, skin-friction coefficient and Reynolds number and, assuming that the variation of temperature with pressure in the atmosphere is known, the relationship between dynamic viscosity and temperature.

It is generally accepted that, for incompressible flow ($M = 0$), the most accurate flat-plate, skin friction relation is that due to von Kármán and Schoenherr[5]. This has been extended to compressible flow over an adiabatic wall by van Driest[6] and, when the Mach number is 0.5, the resulting relation is

$$\frac{0.5482}{\left(C_F^{FP}\right)_{M=0.5}^{1/2}} = ln\left(\left(C_F^{FP}\right)_{M=0.5} R^{FP}\right) - 0.0649, \quad \ldots (24)$$

where the flat-plate Reynolds number, R^{FP}, is based upon speed, atmospheric density and viscosity and the streamwise length of the plate. It is valid for Reynolds numbers in the range 2×10^5 to 1×10^9 and is based upon a fit to an experimental data base that exhibits a variation of $\pm$ 5% relative to the mean line.

In normal atmospheric conditions, the relationship between dynamic viscosity and temperature is adequately represented by Sutherland's Law, i.e.

$$\mu_\infty = 1.458.10^{-6} \frac{(T_\infty)^{1.5}}{(T_\infty + 110.4)} \left(\frac{kg}{m.s} \right), \quad \ldots (25)$$

where the temperature is given in Kelvins.

At any stage in the flight, the aircraft will have a weight that is equal to the take-off value less the weight of the fuel burned up to that point. The crew-controlled variables are speed and altitude, or, since aircraft fly along isobars, speed and static pressure, p_∞, and the problem is to find the combination of Mach number and altitude that gives the absolute minimum fuel burn. This being the case, the Reynolds number becomes a variable and the "optimum" flight conditions occur when

$$d(\eta_o L/D) = \frac{\partial(\eta_o L/D)}{\partial p_\infty} dp_\infty + \frac{\partial(\eta_o L/D)}{\partial M_\infty} dM_\infty = 0 \quad \ldots (26)$$

This equation is satisfied when

$$\frac{\partial(\eta_o L/D)}{\partial p_\infty} = \frac{\partial(\eta_o L/D)}{\partial M_\infty} = 0 \quad \ldots (27)$$

Clearly, for a given aircraft and engine combination, i.e. with aircraft mass, m, reference wing area, S_{ref}, and coefficients ψ_1,ψ_2, and ψ_4 all specified, the optimum pressure level and Mach number can be found by solving Equations (23), (24), (25) and (27) numerically. However, as shown in the next section, a simple and accurate analytic solution can be derived.

4.0 ANALYTIC SOLUTION

Accurate though the skin friction relation given in Equation (24) may be, its implicit form makes it difficult to use in analytic studies. However, for the turbofan powered, transport aircraft considered here[5], the cruise Reynolds numbers lie between 3×10^7 and 3×10^8. Over this reduced range, Equation (24) may be replaced by a simple power law, i.e.

$$\left(C_F^{FP}\right)_{M=0.5} = C_F^{ac} \approx \frac{a}{(R^{ac})^b}, \quad \ldots (28)$$

where a and b are constants having values of 0.0269 and 0.14 respectively. Over the specified Reynolds number range, this gives values that differ from Equation (24) by less than $\pm$0.35% - see Fig. 2.

[5]The aircraft types range from small business jets through to super-jumbo airliners.

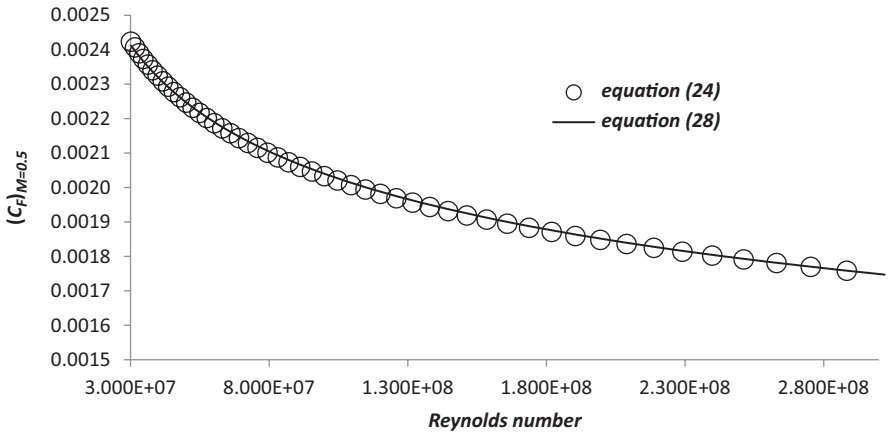

Figure 2. Comparison between the Karman-Schoenherr-van Driest skin friction law for a flat plate at a Mach number of 0.5 and the power-law approximation given in Equation (28).

Consider now the case where the Mach number is constant. Introducing the normalised variables

$$\xi = \frac{C_L}{(C_L)_m^R},\ \chi = \frac{(p_{TP})_{ISA}}{p_\infty}\ \zeta = \frac{M_\infty}{\psi_4} \quad \text{and} \quad \phi = \frac{\mu_\infty a_\infty}{(\mu_{TP} a_{TP})_{ISA}} \qquad \ldots (29)$$

and using Equations (3) and (5), the Reynolds number can be expressed as

$$R^{ac} = \frac{\psi_5 \zeta}{\phi \chi} = \left(\frac{\psi_5 \psi_6}{\phi \zeta C_L}\right)\left(\frac{m}{MTOM}\right), \qquad \ldots (30)$$

where $MTOM$ is the maximum permitted take-off mass, as listed in the aircraft's Type Certificate Data Sheet, e.g. Ref. 7 and both $MTOM$ and S_{ref} have been expressed in non-dimensional form as

$$\psi_5 = \left(\frac{S_{ref}^{1/2} \psi_4 \gamma p_{TP}}{\mu_{TP} a_{TP}}\right)_{ISA} \text{ and } \psi_6 = \left(\frac{MTOM.g}{(\gamma/2)\, p_{TP} \psi_4^2 S_{ref}}\right)_{ISA} \qquad \ldots (31)$$

The normalising quantities are taken to be those at the tropopause (subscript TP) in the International Standard Atmosphere (subscript ISA), i.e. p_∞ is 226.32 hPa and T_∞ is 216.65. A complete description of the International Standard Atmosphere can be found in Ref. 8.

Substituting these variables into Equation (23) and using the relations listed in Appendix A gives

$$(\eta_o L/D) = f_1 \psi_1 \, (C_F)_{ac}^{-\left(\frac{1+\tau}{2}\right)} \left(1 + \frac{A}{2}(\xi - 1)^2 + \frac{B}{6}(\xi - 1)^3\right), \qquad \ldots (32)$$

where

$$f_1 = f_1(\zeta)\,, f_2 = f_2(\zeta)\,, A = A\,(\zeta) \text{ and } B = B(\zeta) \qquad \ldots (33)$$

Differentiating Equation (32) with respect to χ gives

$$\frac{\partial(\eta_o L/D)}{\partial\chi} = f_1\psi_1 (C_F)_{ac}^{-\left(\frac{1+\tau}{2}\right)} \left(\left(\frac{\partial\xi}{\partial\chi}\right)\left(A(\xi-1)+\frac{B}{2}(\xi-1)^2\right)\right.$$
$$\left. -\frac{1}{\chi}\left(\frac{1+\tau}{2}\right)\left(\frac{\chi}{(C_F)_{ac}}\frac{\partial(C_F)_{ac}}{\partial\chi}\right)\left(1+\frac{A}{2}(\xi-1)^2+\frac{B}{6}(\xi-1)^3\right)\right) \quad \ldots(34)$$

Here,

$$\frac{\partial\xi}{\partial\chi} = \left(\frac{\xi}{\chi}\right)\left(1-\left(\frac{1-\tau}{2}\right)\left(\frac{\chi}{(C_F)_{ac}}\frac{\partial(C_F)_{ac}}{\partial\chi}\right)\right) \quad \ldots(35)$$

and, from Equations (28) and (30),

$$\frac{\chi}{C_F^{ac}}\frac{\partial C_F^{ac}}{\partial\chi} = b(1+\Gamma), \quad \ldots(36)$$

where

$$\Gamma = \frac{\chi}{\phi}\frac{d\phi}{d\chi} \quad \ldots(37)$$

The term Γ captures all the effects resulting from vertical temperature variations in the atmosphere.

Hence, at any given Mach number, the maximum, or best, value of $(\eta_o L/D)$ occurs when Equation (34) is equal to zero, i.e.

$$\xi\left(1-\left(\frac{1-\tau}{2}\right)b(1+\Gamma)\right)\left(A(\xi-1)+\frac{B}{2}(\xi-1)^2\right)$$
$$= \left(\frac{1+\tau}{2}\right)b(1+\Gamma)\left(1+\frac{A}{2}(\xi-1)^2+\frac{B}{6}(\xi-1)^3\right) \quad \ldots(38)$$

This is a cubic equation for ξ and the coefficients depend upon Mach number, the relationships linking Reynolds number and Oswald factor to skin friction and the variation of atmospheric temperature with height. If the skin friction is independent of the Reynolds number, i.e. b is zero, then ξ is equal to 1. However, as shown in Equation (28), b is non-zero, but still small. Therefore, expressing the solution in the form

$$\xi_B = \frac{(C_L)_B}{(C_L)_B^R} \approx 1+\Delta_B, \quad \ldots(39)$$

substituting this into Equation (38) and neglecting terms of order Δ^2 and above in comparison to unity, the first order approximate solution is found to be

$$(C_L)_B = \xi_B (C_L)_B^R \approx (1+\Delta_B) f_2\psi_2 \left(C_F^{ac}\right)_B^{\left(\frac{1-\tau}{2}\right)}, \quad \ldots(40)$$

where

$$\Delta_B \approx \frac{b\,(1+\tau)\,(1+\Gamma_B)}{A\,(2-b\,(1-\tau)\,(1+\Gamma_B))} \qquad \ldots(41)$$

Whilst this equation is simple, it is found that for ζ between 0.8 and 1.08, τ between 0.1 and 0.3 and Γ lying in the range ± 1, it can be in error by more than 10%. However, taking b to be 0.14, using Equation (41) as a guide, solving Equation (38) numerically and curve fitting, it is found that

$$\Delta_B \approx \frac{0.07875}{A}\,(1+0.935\tau)\left(1+1.120\Gamma_B+0.120\Gamma_B^2\right) \qquad \ldots(42)$$

This relation is exact when ζ is unity, τ is 0.2 and Γ is zero and differs from the full solution by less than 2% when all parameters have their largest, or smallest, values.

In order to locate the optimum condition, the solution for the best lift coefficient at a given Mach number (Equation 39) is substituted into Equation (32), giving

$$(\eta_o L/D)_B \approx f_1 \psi_1 \left(C_F^{ac}\right)_B^{-\left(\frac{1+\tau}{2}\right)} \left(1+\frac{A}{2}(\Delta_B)^2+\frac{B}{6}(\Delta_B)^3\right) \qquad \ldots(43)$$

For an aircraft with a given mass, this equation is a function of Mach number only and differentiation with respect to ζ gives

$$\frac{\partial(\eta_o L/D)_B}{\partial\zeta} = f_1\psi_1\left(C_F^{ac}\right)_B^{-\left(\frac{1+\tau}{2}\right)}\left(\frac{\Delta_B^3}{6}\frac{dB}{d\zeta}-\frac{\Delta_B^2}{2}\left(1+\Delta_B\frac{B}{A}\right)\frac{dA}{d\zeta}+\right.$$
$$\left.\frac{1}{\zeta}\left(\frac{\zeta}{f_1}\frac{df_1}{d\zeta}-\left(\frac{1+\zeta}{2}\right)\left(\frac{\zeta}{C_F^{ac}}\frac{\delta C_F^{ac}}{\delta\zeta}\right)\right)\left(1+\frac{A}{2}\Delta_B^2+\frac{B}{6}\Delta_B^3\right)\right) \qquad \ldots(44)$$

In addition, using Equations (5), (28), (30) and (37), it can be shown that

$$\frac{\zeta}{C_F^{ac}}\frac{\partial C_F^{ac}}{\partial\zeta} = b\,(1+\Gamma_B)\left(\left(\frac{1+2\Gamma_B}{1+\Gamma_B}\right)+\frac{\zeta}{C_L}\frac{\partial C_L}{\partial\zeta}\right) \qquad \ldots(45)$$

Whilst, from Equation (40),

$$\frac{\zeta}{C_L}\frac{\partial C_L}{\partial\zeta} = \left(\frac{1-\tau}{2}\right)\left(\frac{\zeta}{C_F^{ac}}\frac{\partial C_F^{ac}}{\partial\zeta}\right)+\frac{\zeta}{f_2}\frac{df_2}{d\zeta}-\frac{\Delta_B}{(1+\Delta_B)}\frac{\zeta}{A}\frac{dA}{d\zeta} \qquad \ldots(46)$$

Hence,

$$\left(\frac{1+\tau}{2}\right)\left(\frac{\zeta}{C_F^{ac}}\frac{\delta C_F^{ac}}{\delta\zeta}\right) = \mathrm{A}\Delta_B\left(\left(\frac{1+2\Gamma_B}{1+\Gamma_B}\right)+\frac{\zeta}{f_2}\frac{df_2}{d\zeta}-\frac{\Delta_B}{(1+\Delta_B)}\frac{\zeta}{A}\frac{dA}{d\zeta}\right) \qquad \ldots(47)$$

Substituting Equation (47) into Equation (44), neglecting quantities that are small compared to unity and noting from Equations (A-6) and (A-7) in Appendix A that

$$\frac{dB}{d\zeta} = 2.25\frac{dA}{d\zeta}, \qquad \ldots(48)$$

gives

$$\frac{\partial(\eta_o L/D)_B}{\partial\zeta} \approx f_1\psi_1\left(\frac{1}{C_F^{ac}}\right)^{\left(\frac{1+\tau}{2}\right)}\left(\frac{1}{\zeta}\right)\left(\frac{\zeta}{f_1}\frac{df_1}{d\zeta} - A\Delta_B\left(\left(\frac{1+2\Gamma_B}{1+\Gamma_B}\right)\right.\right.$$
$$\left.\left.+\frac{\zeta}{f_2}\frac{df_2}{d\zeta} - \frac{\Delta_B}{2}\frac{\zeta}{A}\frac{dA}{d\zeta}\left(1-1.25\Delta_B\left(1+0.8\frac{B}{A}\right)\right)\right)\right) \quad \ldots(49)$$

Therefore, the optimum condition occurs when

$$\left(\frac{\zeta}{f_1}\frac{df_1}{d\zeta}\right)_o = (A\Delta)_o\left(\left(\frac{1+2\Gamma_o}{1+\Gamma_o}\right) + \left(\frac{\zeta}{f_2}\frac{df_2}{d\zeta}\right)_o\right.$$
$$\left.-\left(\frac{\Delta}{2}\frac{\zeta}{A}\frac{dA}{d\zeta}\right)_o\left(1-1.25\Delta_o\left(1+0.8\left(\frac{B}{A}\right)_o\right)\right)\right) \quad \ldots(50)$$

An approximate solution to this equation may be obtained by setting

$$\zeta_o = \frac{M_o}{\psi_4} = 1+\varepsilon \quad \ldots(51)$$

and expressing the parameters as power series in ascending powers of ε, i.e. from Equations (A-5), (A-8), (A-9) and (A-12) in Appendix A,

$$\left(\frac{\zeta}{f_1}\frac{df_1}{d\zeta}\right)_o \approx -11.79\varepsilon - 10.71\varepsilon^2 + \ldots., \quad \ldots(52)$$

$$\left(\frac{\Delta}{2}\frac{\zeta}{A}\frac{dA}{d\zeta}\right)_o \approx -\frac{3}{(2.675)^2}(A\Delta)_o\left(1+36.51\varepsilon - 218.6\varepsilon^2 + \ldots.\right), \quad \ldots(53)$$

$$\left(\frac{B}{A}\right)_o \approx 1.0350\left(1+2.633\varepsilon + 46.75\varepsilon^2 + \ldots.\right) \quad \ldots(54)$$

and

$$\left(\frac{\zeta}{f_2}\frac{df_2}{d\zeta}\right)_o \approx -\left(1+22.92\varepsilon + 262.2\varepsilon^2 + \ldots.\right) \quad \ldots(55)$$

By using Equations (51)–(55), Equation (50) becomes a quadratic for ε. If $(A\Delta)_o$ is small, ignoring terms of order ε^2 and above and using Equation (41), the first order, approximate solution to Equation (50) is given by

$$\varepsilon \approx -0.085(A\Delta)_o\left(\frac{\Gamma_o}{1+\Gamma_o}\right) \approx -0.085\frac{b\,(1+\tau)\,\Gamma_o}{(2-b\,(1-\tau)\,(1+\Gamma_o))} \quad \ldots(56)$$

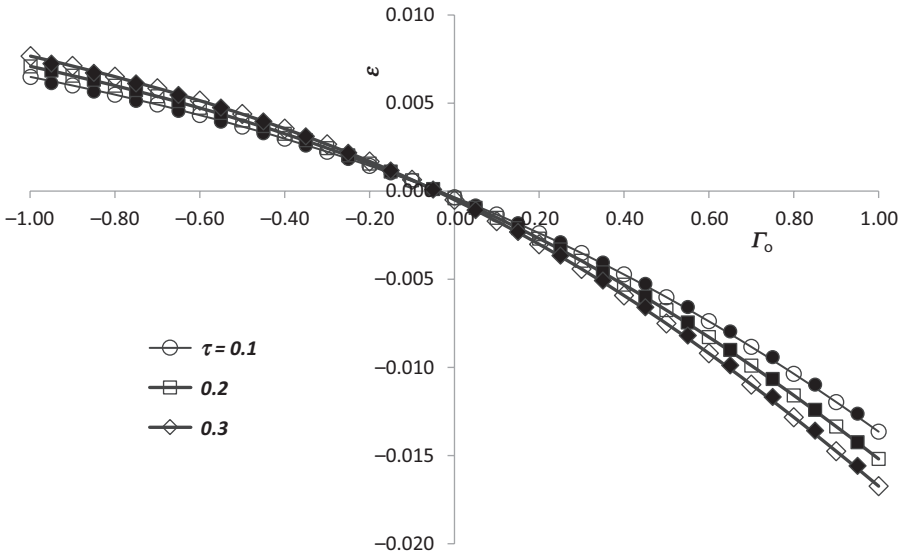

Figure 3. The variation of ε with Γ_o and τ. Open symbols show the numerical solutions to Equations (38) and (50), whilst closed symbols are the estimates obtained from Equation (57).

However, whilst this result indicates the structure of the solution, its accuracy reduces significantly as Γ_o increases. To correct this shortcoming, Equations (38) and (50) can be solved simultaneously, using simple numerical iteration, and the results for b equal to 0.14, τ lying in the range 0.1 to 0.3 and values of Γ_o between $\pm$ 1 are shown in Fig. 3. These can then be used to develop an approximate solution in which ε is expressed as a series in ascending powers of Γ_o, whose coefficients depend upon τ. The result is

$$\varepsilon \approx -0.000260\,(1+2.825\tau)\,(1+30.18\,(1-0.66\tau)\,\Gamma_o + 10.27\,(1-0.57\tau)\,\Gamma_o^2 + 1.91\,(1-1.78\tau)\,\Gamma_o^3) \quad \ldots(57)$$

This is exact when τ is 0.2 and Γ is zero and differs from the full solution by less than 2.5% when all parameters have their extreme values.

The corresponding results for Δ_o are presented in Fig. 4, and these may be represented, approximately, by the function

$$\Delta_o \approx -0.02946\,(1+0.956\tau)\,\left(1+1.14\Gamma_o+0.14\Gamma_o^2\right) \quad \ldots(58)$$

Once again, this expression is exact when τ is 0.2 and Γ is zero and differs from the full solution by less than 2% for all other parameter combinations.

4.1 Approximate relations for Reynolds number and Γ

As can be seen from Equation (30), the temperature dependent quantities that influence Reynolds number are confined to the term ϕ and, since ϕ involves the product of dynamic viscosity and the speed of sound, it is a function of temperature alone. For air temperatures in

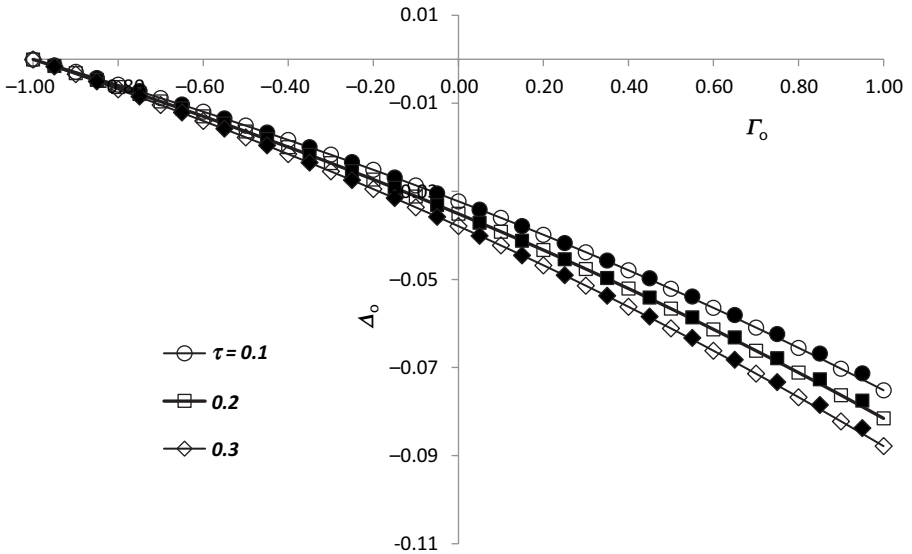

Figure 4. The variation of Δ_o with Γ_o and τ. Open symbols show the numerical solution to Equations (38) and (50), whilst closed symbols are the estimates obtained from Equation (58).

the range 175K to 265K, Equation (25) can be used to show that ϕ may be represented by the simple power law

$$\frac{\mu_\infty a_\infty}{(\mu_{TP} a_{TP})_{ISA}} = \phi \approx \left(\frac{T_\infty}{(T_{TP})_{ISA}} \right)^{1.34}, \qquad \ldots (59)$$

to an accuracy of better than ±0.5% - see Fig. 5. Hence,

$$\frac{T_\infty}{\phi} \frac{d\phi}{dT_\infty} \approx 1.34 \qquad \ldots (60)$$

and this result is accurate to better than ± 3.5% over the same temperature range.

If the static temperature, T_∞, in a general atmosphere is now written as $(T_\infty)_{ISA}$ plus ΔT, where ΔT is a function of altitude and is generally small compared to $(T_\infty)_{ISA}$, then

$$\frac{T_\infty}{(T_{TP})_{ISA}} = \left(\frac{T_\infty}{T_{TP}} \right)_{ISA} + \frac{\Delta T}{(T_{TP})_{ISA}} = \overline{T} + \overline{\Delta T} \qquad \ldots (61)$$

Hence,

$$\phi \approx \left(1 + 1.34 \frac{\overline{\Delta T}}{\overline{T}} \right) \overline{T}^{1.34} \qquad \ldots (62)$$

and, in the vicinity of the 226.32 hPa isobar (*ISA* tropopause) where $\overline{T}$ is close to unity, the simplified expression,

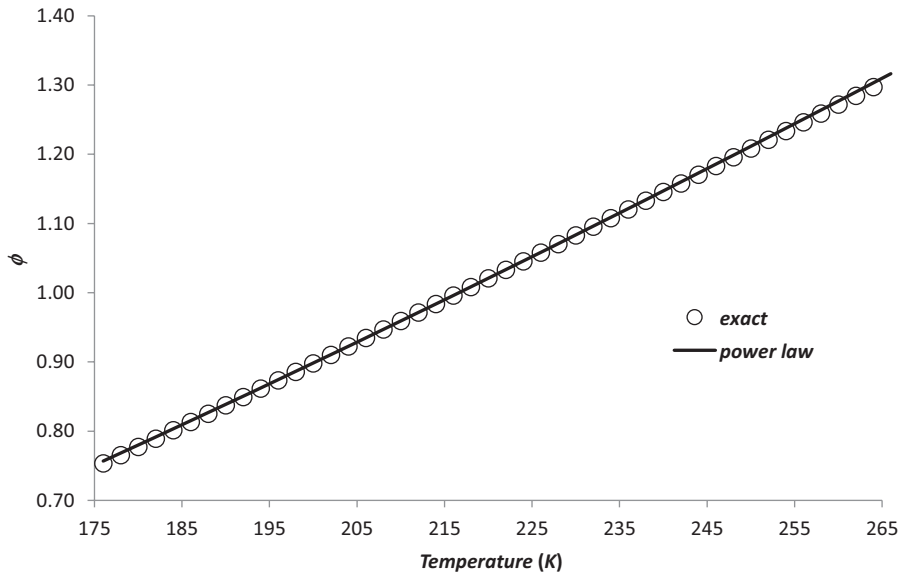

Figure 5. The variation of ϕ with temperature and comparison with the power-law approximation given in Equation (59).

$$\phi \approx \left(1 + 1.34\overline{\Delta T}\right) \overline{T}^{1.34}, \qquad \ldots (63)$$

may be used. For attitudes above 28,000 feet, Equation (63) is found to be accurate to better than $\pm$ 2% for values of $\overline{\Delta T}$ in the range $\pm$ 0.15.

In the International Standard Atmosphere[8], the troposphere and the stratosphere are regions within which the local, vertical temperature gradient, or "lapse" rate, is constant. This gradient is usually expressed as the derivative of temperature with respect to the geopotential altitude[6], h, designated here as L_h and which has units of K/m. In a general atmosphere, temperature, pressure and altitude are linked by the hydrostatic equation, i.e.

$$dp = -\rho g_{SL} dh, \qquad \ldots (64)$$

where ρ is the local air density and g_{SL} is the acceleration due to gravity at sea level. Hence, for the *ISA*,

$$\overline{T} = \chi^{\omega}, \qquad \ldots (65)$$

where the exponent ω is a constant given by

$$\omega = \frac{\Re L_h}{g_{SL}} \qquad \ldots (66)$$

[6]The geopotential altitude is the gravitational potential energy per unit mass at a given geometric altitude, measured relative to mean sea level, divided by the acceleration due to gravity at sea level.

and $\Re$ is the gas constant for air. Therefore, using Equations (5), (31), (63) and (65),

$$\phi \approx \left(1 + 1.34\overline{\Delta T}\right) \chi^{1.34\omega} = \left(1 + 1.34\overline{\Delta T}\right) \left(\frac{\psi_6}{C_L \zeta^2} \left(\frac{m}{MTOM}\right)\right)^{1-i}, \quad \ldots (67)$$

where

$$\iota = 1 + 1.34\omega \quad \ldots (68)$$

In the *ISA* troposphere, where χ is less than, or equal to, unity, L_h is -0.0065K/m. Hence, ω is -0.19026 and i is 0.74505. In the *ISA* stratosphere, χ is greater than unity and, since both L_h and ω are zero, i is equal to one.

Hence, from Equations (30), (31) and (67), the general expression for Reynolds number is

$$R^{ac} \approx \frac{\psi_5}{\left(1 + 1.34\overline{\Delta T}\right)} \zeta^{(1-2i)} \left(\frac{\psi_6}{C_L} \left(\frac{m}{MTOM}\right)\right)^{i} = \frac{\psi_5}{\left(1 + 1.34\overline{\Delta T}\right)} \left(\frac{\zeta}{\chi^i}\right) \quad \ldots (69)$$

In aircraft operations, to guarantee safe vertical separation of traffic, altitude is replaced by the non-dimensional "Flight Level", *FL*, which, by international agreement, is defined as the geopotential altitude, in units of feet, in the International Standard Atmosphere at the same value of the static pressure, p_∞, divided by 100 feet. This means that the Flight Level only depends upon the atmospheric static pressure. Therefore, using the relations given in Ref. 8, if χ is less than, or equal to, 1,

$$FL = 1454.42 \left(1 - 0.751865(\chi)^{-0.19026}\right) \text{ and } i = 0.74505, \quad \ldots (70)$$

whilst, if χ is greater than 1,

$$FL = 360.8924 + 208.058 ln\,(\chi) \text{ and } i = 1 \quad \ldots (71)$$

It is important to note that, if Flight Level is used to describe an aircraft's altitude, then, by definition, Equations (70) and (71) are true for all atmospheres.

It follows that the variation of $\mathrm{d}\chi/\mathrm{d}FL$ with Flight Level is also the same in all atmospheres and from Equation (64),

$$\left(\frac{\chi}{FL}\frac{dFL}{d\chi}\right) = \left(\frac{\chi}{FL}\frac{dFL}{d\chi}\right)_{ISA} = \left(\frac{\Re(T_{TP})_{ISA}}{30.48 g_{SL}}\right)\left(\frac{\overline{T}}{FL}\right) = 208.06\left(\frac{\overline{T}}{FL}\right) \quad \ldots (72)$$

However, the variation of temperature with pressure and, hence, the variation of $dT_\infty/\mathrm{d}FL$ with Flight Level depend upon the actual atmospheric conditions. Therefore, in general, from Equations (37), (60) and (72)

$$\Gamma = \left(\frac{T_\infty}{\phi}\frac{d\phi}{dT_\infty}\right)\left(\frac{\chi}{FL}\frac{dFL}{d\chi}\right)\left(\frac{FL}{T_\infty}\frac{dT_\infty}{dFL}\right) \approx 278.8\left(\frac{\overline{T}}{FL}\right)\left(\frac{FL}{T_\infty}\frac{dT_\infty}{dFL}\right) \quad \ldots (73)$$

and, from Equation (61),

$$\left(\frac{FL}{T_\infty}\frac{dT_\infty}{dFL}\right) = \frac{FL}{\left(\overline{T}+\overline{\Delta T}\right)}\left(\frac{d\left(\overline{T}+\overline{\Delta T}\right)}{dFL}\right) = \frac{\overline{T}}{\left(\overline{T}+\overline{\Delta T}\right)}\left(\frac{FL}{\overline{T}}\right)\frac{1}{(T_{TP})_{ISA}}\frac{dT_\infty}{dFL} \quad \ldots(74)$$

Hence,

$$\Gamma \approx 278.8\left(\frac{\overline{T}}{\overline{T}+\overline{\Delta T}}\right)LR, \quad \ldots(75)$$

where LR is the non-dimensional, temperature change per Flight Level defined as

$$LR = \frac{1}{(T_{TP})_{ISA}}\frac{dT_\infty}{dFL} = 0.1407L_h \quad \ldots(76)$$

This result is valid for all Flight Levels. However, in the vicinity of FL 360, where $\overline{T}$ is close to unity,

$$\Gamma \approx 277\left(1-\overline{\Delta T}\right)LR \quad \ldots(77)$$

Here, the constant of proportionality has been adjusted so that, for Flight Levels greater than 280, this expression is accurate to better than ± 3.5%, when $\overline{\Delta T}$ and LR are in the range ± 0.15 and ± 0.0045, respectively.

In the International Standard Atmosphere, Γ is approximately -0.254 in the upper troposphere and zero in the stratosphere. However, the *ISA* is a reference scenario based upon long-time average observations and, on short time scales, the variation of temperature with FL may differ significantly from the *ISA* values. An example of an "instantaneous" vertical temperature profile is shown in Fig. 6. Since Equation (77) is valid for all atmospheric conditions, Γ can be evaluated from the data given in Fig. 6 and the results are shown in Table 1. The first two columns give the observed variation of temperature with pressure, whilst the next eight columns contain the derived quantities and the estimated value of Γ is given in the last column.

4.2 The optimum conditions

For an aircraft of specified mass, at any given Mach number, the value of the Reynolds number at which $(\eta_o L/D)$ has its best (local maximum) value is obtained by combining Equations (28), (40) and (69), i.e.

$$R_B^{ac} \approx G_1\psi_5\left(\zeta^{(1-2\iota_B)}\left(\frac{1}{\psi_7 f_2}\left(\frac{m}{MTOM}\right)\right)^{\iota_B}\right)^{\kappa_B}, \quad \ldots(78)$$

where

$$G_1 = \left(\left(1+1.34\overline{\Delta T}_B\right)(1+\Delta_B)^{i_B}\right)^{-\kappa_B}, \quad \ldots(79)$$

$$\kappa_B = \left(\frac{2}{2-i_B b\,(1-\tau)}\right) \quad \ldots(80)$$

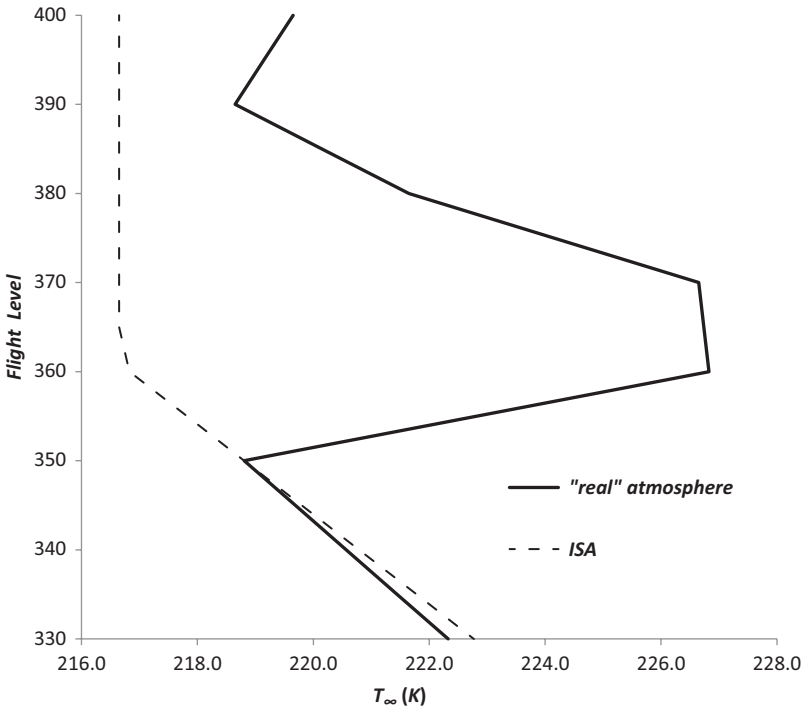

Figure 6. An example of an observed variation of atmospheric temperature with Flight Level compared with that in the International Standard Atmosphere.

and

$$\psi_7 = \frac{\psi_2}{\psi_6}\left(\frac{a}{\psi_5^b}\right)^{\left(\frac{1-\tau}{2}\right)} \qquad \ldots(81)$$

The value of the Reynolds number when $(\eta_o L/D)$ has its optimum value depends upon M_o, which comes from a combination of Equations (51) and (57). With the Mach number at this optimum value, approximations for $f_{1,} f_2$ and A can be obtained from Equations (A-5), (A-8) and (A-12), i.e.

$$(f_1)_o \approx 1 - 5.897\varepsilon^2 + \ldots, \qquad \ldots(82)$$

$$(f_2)_o \approx 1 - \varepsilon - 10.46\varepsilon^2 + \ldots \qquad \ldots(83)$$

and

$$A_o \approx -2.675\left(1 + 2.243\varepsilon + 44.86\varepsilon^2 + \ldots\right) \qquad \ldots(84)$$

Substituting these results into Equations (78) and (79), expanding and neglecting the products of small quantities, the value of the Reynolds number at the optimum condition is given by

Table 1
An example of a typical variation of atmospheric temperature with pressure and the processing steps to estimate Γ

p_∞ (Pa)	T_∞ (K)	FL	ι	dT_∞/dFL (K)	$(T_\infty)_{ISA}$ (K)	ΔT (K)	$\overline{\Delta T}$	LR	Γ_{exact}	Γ_{est}	% diff
26201	222.33	330	0.74505	−0.176	222.77	−0.44	−0.0021	−8.12 E-04	−0.225	−0.225	0.0
25594	221.45	335	0.74505	−0.176	221.78	−0.33	−0.0015	−8.12 E-04	−0.225	−0.225	−0.1
24999	220.57	340	0.74505	−0.176	220.79	−0.22	−0.0010	−8.12 E-04	−0.226	−0.225	−0.2
24415	219.69	345	0.74505	−0.176	219.80	−0.11	−0.0005	−8.12 E-04	−0.226	−0.225	−0.2
23842	218.81	350	0.74505	0.802	218.81	0.00	0.0000	3.70 E-03	1.025	1.025	0.0
23280	222.82	355	0.74505	0.802	217.82	5.00	0.0231	3.70 E-03	1.002	1.001	−0.1
22729	226.83	360	0.74505	−0.018	216.83	10.00	0.0462	−8.17 E-05	−0.022	−0.022	0.1
22190	226.74	365	1.00000	−0.018	216.65	10.09	0.0466	−8.12 E-05	−0.022	−0.021	−0.5
21663	226.65	370	1.00000	−0.500	216.65	10.00	0.0462	−2.31 E-03	−0.610	−0.610	−0.1
21148	224.15	375	1.00000	−0.500	216.65	7.50	0.0346	−2.31 E-03	−0.617	−0.617	0.0
20646	221.65	380	1.00000	−0.300	216.65	5.00	0.0231	−1.38 E-03	−0.376	−0.375	−0.3
20156	220.15	385	1.00000	−0.300	216.65	3.50	0.0162	−1.38 E-03	−0.378	−0.377	−0.3
19677	218.65	390	1.00000	0.100	216.65	2.00	0.0092	4.62 E-04	0.127	0.127	−0.3
19210	219.15	395	1.00000	0.100	216.65	2.50	0.0115	4.62 E-04	0.127	0.126	−0.3
18754	219.65	400	1.00000	0.100	216.65	3.00	0.0138	4.62 E-04	0.127	0.126	−0.3

$$R_o^{ac} \approx G_2 \psi_5 \left(\frac{1}{\psi_7} \left(\frac{m}{MTOM} \right) \right)^{\iota_o \kappa_o}, \quad \ldots (85)$$

where

$$G_2 \approx \left(\left(1 + 1.34 \overline{\Delta T}_o \right) \left((1 + \Delta_o)\,(1 - \varepsilon) \right)^{i_o} (1 + \varepsilon)^{(2i_o - 1)} \right)^{-\kappa_o} \quad \ldots (86)$$

and

$$\kappa_o = \left(\frac{2}{2 - i_o b\,(1 - \tau)} \right) \quad \ldots (87)$$

For maximum accuracy, G_2 is evaluated directly using Equations (57) and (58). Unfortunately, the form of Equation (86) does not yield any clear insight as to how G_2 relates to the various aircraft and atmospheric parameters. However, by expansion, approximation and use of Equation (77), (86) may be re-cast in terms of the key parameters[7], i.e.

$$\begin{aligned} G_2 \approx {} & (1 + 0.033\,(1 + 0.89\tau)) \times \left(1 - 0.040\,(1 - i_o) - 1.47 \overline{\Delta T}_o \left(1 - 1.40 \overline{\Delta T}_o \right) \right. \\ & \left. + 16.35\,(i_0 - 0.235) \left(1 - \overline{\Delta T}_o \right) LR_o \right) \end{aligned} \quad \ldots (88)$$

Here, the first bracketed term contains the result for cruise in the *ISA* stratosphere, i.e. where $FL > 360.9$, $p_\infty < 226.32$ hPa, i_o is unity and ΔT and LR are both zero, whilst the second gives a correction to allow for the actual atmospheric conditions being encountered. The accuracy of the correction term deceases monotonically as both $\overline{\Delta T}$ and LR get either larger, or smaller, with the maximum deviation from Equation (86) being ± 2% for values of τ between 0.1 and 0.3 and $\overline{\Delta T}_o$ and LR_o lying in the ranges ± 0.15 and ± 0.0045, respectively.

Having found the Reynolds number, the mean skin-friction coefficient at the optimum condition follows from Equation (28), i.e.

$$\left(C_F^{ac} \right)_o = \frac{a}{\left(R_o^{ac} \right)^b} \approx G_3 \left(\frac{a}{\psi_5^b} \right) \left(\psi_7 \left(\frac{MTOM}{m} \right) \right)^{b \iota_o \kappa_o}, \quad \ldots (89)$$

where, using Equation (88) and neglecting small quantities,

$$G_3 = (G_2)^{-b} \approx 0.995 \left(1 + 0.20 \overline{\Delta T}_o - 1.75 \left(1 - \overline{\Delta T}_o \right) LR_o \right) \quad \ldots (90)$$

Therefore, the lift coefficient at the optimum condition is given by combining Equations (40) and (89), i.e.

$$(C_L)_o = (1 + \Delta_o)\,(f_2)_o \psi_2 \left(C_F^{ac} \right)_o^{\left(\frac{1-\tau}{2} \right)} = G_4 \psi_2 \left(\left(\frac{a}{\psi_5^b} \right) \left(\psi_7 \left(\frac{MTOM}{m} \right) \right)^{b \iota_o \kappa_o} \right)^{\left(\frac{1-\tau}{2} \right)}, \quad \ldots (91)$$

[7] Whist formal, asymptotic approximation rules are used to establish the basic form of the equation, the final values of the coefficients are determined by best fits to the data over the specified ranges.

where

$$G_4 = (1 + \Delta_o)\,(f_2)_o (G_3)^{\left(\frac{1-\tau}{2}\right)} \qquad \ldots (92)$$

The approximate form of this relation is

$$G_4 \approx 0.9685\,(1 - 0.027\tau)\left(1 + 0.080\overline{\Delta T}_o - 9.70\left(1 - \overline{\Delta T}_o\right) LR_o\right), \qquad \ldots (93)$$

which is within ±1% of the full solution for the same parameter range as Equation (88).

Finally, using Equation (43) and (89), the optimum value of $(\eta_o L/D)$ is

$$(\eta_o L/D)_o = (f_1)_o \psi_1 \left(C_F^{ac}\right)_o^{-\left(\frac{1+\tau}{2}\right)} = G_5 \psi_1 \left(\left(\frac{\psi_5^b}{a}\right)\left(\frac{1}{\psi_7}\left(\frac{m}{MTOM}\right)\right)^{b\iota_o\kappa_o}\right)^{\left(\frac{1+\tau}{2}\right)}, \qquad \ldots (94)$$

where

$$G_5 = (f_1)_o \left(1 + \frac{A_o}{2}\Delta_o^2 + \frac{B_o}{6}\Delta_o^3\right)\left(\frac{1}{G_3}\right)^{\left(\frac{1+\tau}{2}\right)} \qquad \ldots (95)$$

and

$$G_5 \approx 1 - 0.13\overline{\Delta T}_o, \qquad \ldots (96)$$

which is found to be accurate to ±0.5%. It is important to note that the influence of lapse rate on $(\eta_o L/D)_o$ is very small and negligible in most cases of practical interest.

The value of χ for optimum $(\eta_o L/D)$ comes from Equations (5), (31), (51) and (91), i.e.

$$\chi_o \approx \frac{(C_L)_o}{\psi_6}(1+\varepsilon)^2\left(\frac{MTOM}{m}\right) = G_6\left(\psi_7\left(\frac{MTOM}{m}\right)\right)^{\kappa_o}, \qquad \ldots (97)$$

where

$$G_6 = G_4(1+\varepsilon)^2 \qquad \ldots (98)$$

or, in approximate form,

$$G_6 \approx 0.968\,(1 - 0.0285\tau)\left(1 + 0.079\overline{\Delta T}_o - 13.0\,(1 + 0.99\tau)\left(1 - \overline{\Delta T}_o\right) LR_o\right) \qquad \ldots (99)$$

Since both $\overline{\Delta T}$ and LR depend upon χ, Equation (97) is implicit. However, for a given atmosphere, the variations of ι, $\overline{\Delta T}$, LR and Γ with χ are known; see the example given in Table 1. Therefore, Equation (97) can be inverted to give an explicit relation for the mass ratio that gives the optimum fuel burn at a specified value of χ or, via Equations (70) and (71), at a specified Flight Level, i.e.

$$\left(\frac{m}{MTOM}\right)_o = \psi_7\left(\frac{G_6}{\chi}\right)^{\frac{1}{\kappa}} \approx \psi_7\left(\frac{1 + 0.079\overline{\Delta T} - 13.0\,(1 + 0.99\tau)\left(1 - \overline{\Delta T}\right) LR}{1.033\,(1 + 0.0285\tau)\chi}\right)^{\frac{1}{\kappa}}, \qquad \ldots (100)$$

where

$$\kappa = \kappa(\chi) = \left(\frac{2}{2 - ib\,(1 - \tau)} \right) \qquad \ldots (101)$$

In general, Equation (100) is single valued. However, at a point of lapse rate discontinuity, there are two solutions. This may be illustrated by using the example of the International Standard Atmosphere, which has a lapse rate discontinuity at the tropopause ($\chi = 1$). In this case, if χ approaches unity from below, i.e. the aircraft is climbing though the troposphere, where i is 0.74505 and LR is −0.0009145 (L_h is −0.0065 K/m), at the tropopause,

$$\left(\frac{m}{MTOM} \right)_{\chi_o = 1} \approx 0.980\,(1 - 0.016\tau)\psi_7 \qquad \ldots (102)$$

Conversely, if the same point is approached from above, i.e. by descending through the stratosphere, where i is unity and LR is zero,

$$\left(\frac{m}{MTOM} \right)_{\chi_o = 1} \approx 0.970\,(1 - 0.027\tau)\psi_7 \qquad \ldots (103)$$

Between these two mass values, the optimum Flight Level is constant, but the optimum Mach number and $(\eta_o L/D)_o$ both vary. The change in M_o is small and depends only upon the discontinuous change in γ. However, as seen in Equations (94) and (96), $(\eta_o L/D)_o$ varies continuously with mass and, since the atmospheric temperature is also continuous, it may be treated as a continuous function to a very good approximation. For flight operations, the change in Mach number between the two mass values would follow a particular profile. Whist this cannot be determined from the theory and in the absence of any other information, for the purposes of this paper, it will be assumed that it is directly proportional to the aircraft mass. In practise, viscosity prevents true discontinuities. Nevertheless, in those regions of the atmosphere where the lapse rate varies very rapidly with altitude, the optimum Flight Level will be almost independent of the aircraft mass.

An important consequence of the existence of two solutions at a point of lapse rate discontinuity is that, if the vertical temperature profile contains more than one discontinuity, Equation (97) may have multiple solutions at a given mass ratio. If this is the case, whilst each solution corresponds to a local maximum, one will have the highest, or optimum, value of $(\eta_o L/D)$. This optimum is found by substituting the resulting χ_o and $(m/MTOM)$ solution pairs into Equation (94) and comparing the results. Therefore, some care needs to be exercised when using Equations (97) and (100) to make sure that all the solutions have been found and the true optimum has been identified.

Continuing with the ISA example, if the mass ratio is greater than, or equal to, the value given by Equation (102), the optimum altitude lies in the troposphere and χ_o is found from Equations (97) and (99), i.e.

$$\chi_o \approx 0.980\,(1 - 0.017\tau) \left(\psi_7 \left(\frac{MTOM}{m} \right) \right)^{1.052(1 - 0.050\tau)} \qquad \ldots (104)$$

The optimum Flight Level follows directly from Equation (70), with the optimum Mach number coming from Equations (51), (57) and (77), i.e.

$$M_o \approx 1.0016\,(1 + 0.0032\tau)\,\psi_4 \qquad \ldots(105)$$

The optimum lift coefficient comes from Equations (91) and (93), i.e.

$$(C_L)_o \approx 0.977\,(1 - 0.027\tau)\,\psi_2\left(\frac{a}{\psi_5^b}\right)^{\left(\frac{1-\tau}{2}\right)}\left(\psi_7\left(\frac{MTOM}{m}\right)\right)^{0.055(1-1.050\tau)} \qquad \ldots(106)$$

and, finally, the optimum value of $(\eta_o L/D)$ is obtained from Equations (94) and (96)

$$(\eta_o L/D)_o \approx \psi_1\left(\frac{\psi_5^b}{a}\right)^{\left(\frac{1+\tau}{2}\right)}\left(\frac{1}{\psi_7}\left(\frac{m}{MTOM}\right)\right)^{0.055(1+0.950\tau)} \qquad \ldots(107)$$

Conversely, if the mass ratio is less than the value from Equation (102), the optimum altitude must lie in the stratosphere. Hence,

$$\chi_o \approx 0.968\,(1 - 0.0285\tau)\left(\psi_7\left(\frac{MTOM}{m}\right)\right)^{1.070(1-0.065\tau)} \qquad \ldots(108)$$

and the optimum Flight level comes from Equation (71). The optimum Mach number is

$$M_o \approx 0.9997\,(1 - 0.0007\tau)\,\psi_4, \qquad \ldots(109)$$

the optimum lift coefficient is

$$(C_L)_o \approx 0.9685\,(1 - 0.027\tau)\,\psi_2\left(\frac{a}{\psi_5^b}\right)^{\left(\frac{1-\tau}{2}\right)}\left(\psi_7\left(\frac{MTOM}{m}\right)\right)^{0.075(1-1.065\tau)} \qquad \ldots(110)$$

and the optimum value of $(\eta_o L/D)$ is

$$(\eta_o L/D)_o \approx \psi_1\left(\frac{\psi_5^b}{a}\right)^{\left(\frac{1+\tau}{2}\right)}\left(\frac{1}{\psi_7}\left(\frac{m}{MTOM}\right)\right)^{0.075(1+0.935\tau)} \qquad \ldots(111)$$

In summary, Equations (85)–(100) provide a complete solution to the problem of determining the optimum $(\eta_o L/D)$ and the values of Mach number and Flight Level at which it occurs for an aircraft at a given mass flying in a general atmosphere. For highest accuracy, the coefficients G_2 to G_6 are evaluated from Equations (86), (90), (92), (95) and (98) using the results from Equations (57) and (58). However, the approximate relations given in Equations (88), (90), (93), (96) and (99) will be sufficient for most practical purposes.

When using the method in situations where the vertical temperature profile is complex, e.g. as in the example given in Fig. 6, the first step is to characterise the atmospheric temperature variation, i.e. to construct the corresponding Table 1. The second step is to use Equations (100), (70) and (71) to determine how the mass ratio for optimum $(\eta_o L/D)$ varies with the Flight Level. If this reveals that there is more than one value of χ for a given value of $(m/MTOM)_o$, i.e. Equation (97) has multiple solutions, Equation (94) is used to identify the Flight Level that has the largest $(\eta_o L/D)_o$ for that mass ratio and the other solutions are

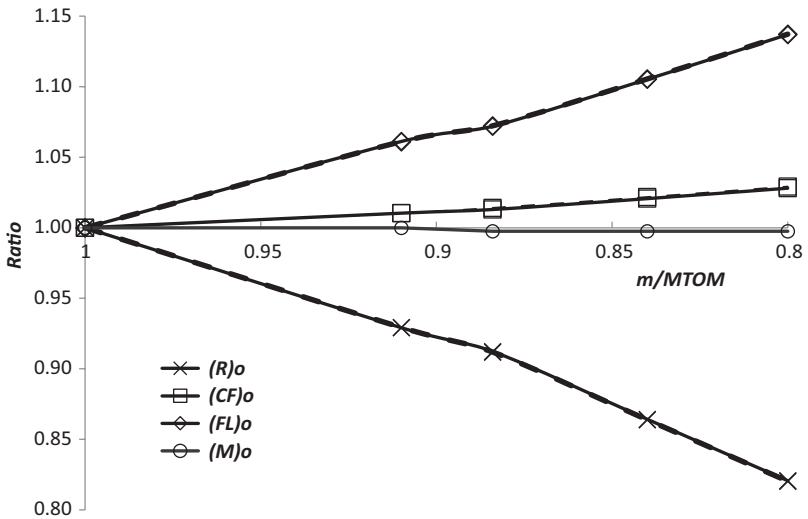

Figure 7. The variation of normalised R_o, $(C_F)_o$, $(FL)_o$ and M_o with aircraft mass under *ISA* conditions. Solid lines indicate numerical values, whilst dashed lines are the approximate solution.

discarded. Therefore, for a specified mass ratio, with $(FL)_o$ and, hence, ι_o, κ_o, LR_o, $\overline{\Delta T}_o$ and Γ_o now established, $(\eta_o L/D)_o$ follows from Equation (94), whilst the corresponding values of the cruise Mach number, M_o, and the lift coefficient, $(C_L)_o$, and come from Equations (51), (57), (58) and (91).

4.3 Comparison with numerical solutions

In order to assess the accuracy of the approximate method, sample cases are compared with accurate numerical solutions to Equations (23) to (27) for an aircraft where ψ_1, ψ_2, ψ_4, ψ_5, ψ_6 and τ have values of 0.17, 6.56, 0.812, 1.27×10^8, 0.57 and 0.19, respectively,. This parameter set is representative of a typical, modern, long-range, wide-bodied aircraft. The results are presented in Figs 7–10.

The variation of Reynolds number, skin-friction coefficient, Flight Level and Mach number with mass ratio when $(\eta_o L/D)$ has its optimum value and the aircraft is flying in *ISA* conditions is shown in Fig. 7. The change in slope between an $(m/MTOM)$ of 0.91 and 0.885 is due to the discontinuity in the lapse rate at the tropopause, as already described. The strongest dependency is exhibited by the Reynolds number, which decreases as the aircraft mass reduces. This means that the skin friction must rise slowly as mass reduces, whilst the optimum cruise altitude increases. The optimum Mach number decreases by 0.25% as the aircraft passes through the tropopause. In all cases, the approximate solutions are found to be very close to the numerical results with maximum differences being less than about 0.2%.

Figure 8 gives the corresponding results for lift coefficient and $(\eta_o L/D)$ at the optimum condition. The variation of $(C_L)_o$ with mass is very small and the effect of the discontinuous lapse rate is clearly visible. The difference between the numerical and the approximate solutions is less than about 0.25%. The optimum value of $(\eta_o L/D)$ also decreases as the mass decreases. The reduction is small, but, in terms of aircraft operations, it is significant. For example, if, on a long route, the fuel to be consumed is 20% of the take-off mass, $(\eta_o L/D)_o$ will decrease

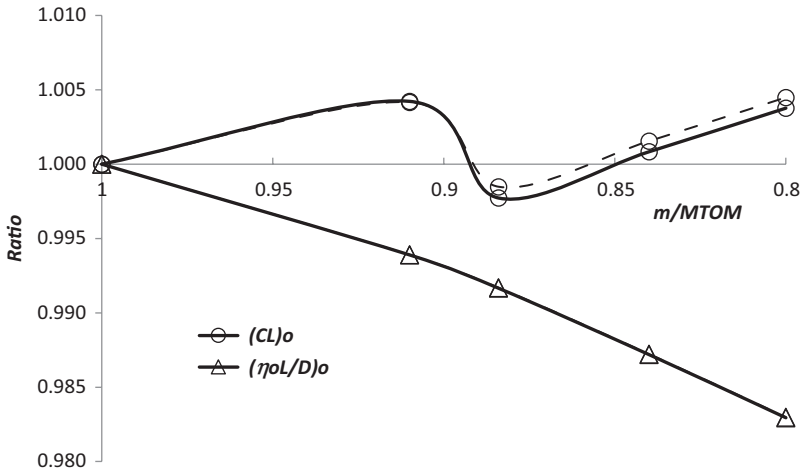

Figure 8. The variation of normalised $(C_L)_o$ and $(\eta_o L/D)_o$ with aircraft mass under *ISA* conditions. Solid lines indicate numerical values, whilst dashed lines are the approximate solution.

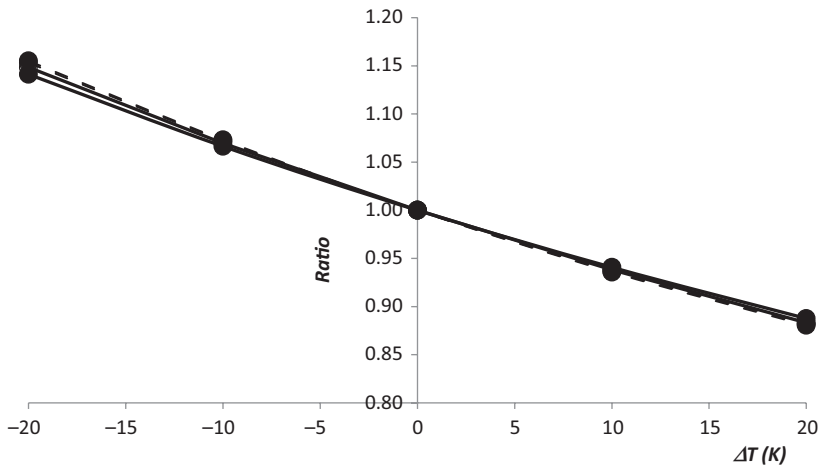

Figure 9. The variation of normalised R_o with temperature deviation from *ISA*. Solid lines indicate numerical values, whilst dashed lines indicate the approximate solution. Solid symbols are for an (*m*/*MTOM*) of 1.0, whilst, for open symbols, (*m*/*MTOM*) = 0.8.

by 2% over the course of the flight and this will have a corresponding adverse effect on the fuel burn rate, see Equation (1).

The variation of optimum Reynolds number with static temperature deviation from the *ISA* values, for two values of the mass ratio, is shown in Fig. 9. This effect is driven by the relationship between static temperature and viscosity, with Reynolds number decreasing as the local temperature increases. A rise of 10K relative to *ISA* reduces R_o by 6.5%. The variations of the skin-friction coefficient, lift coefficient, $(\eta_o L/D)$ and Flight Level at the optimum condition with ΔT are given in Fig. 10. Compared to the influence of temperature on the optimum Reynolds number, these effects are small. The skin-friction coefficient, the lift coefficient and the Flight Level all increase with increasing temperature, with skin friction showing the

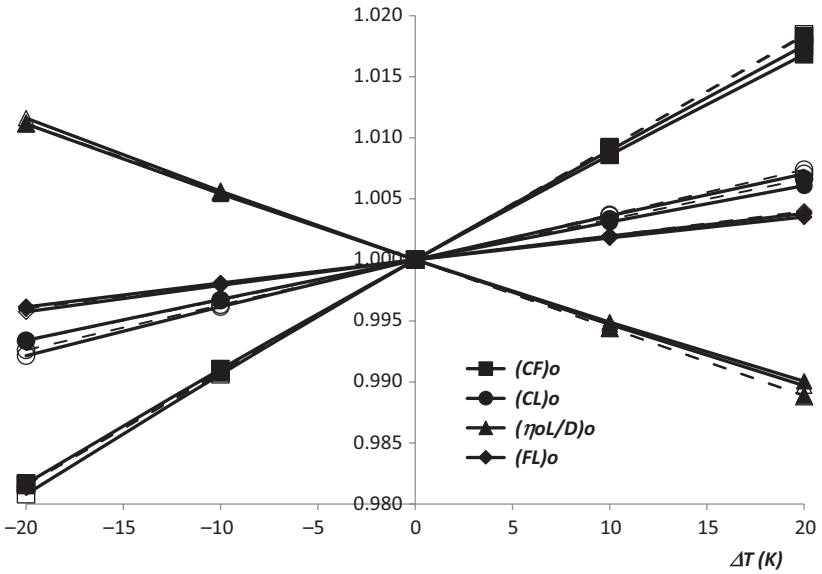

Figure 10. The variation of normalised $(C_F)_o$, $(C_L)_o$, $(\eta_o L/D)_o$, and $(FL)_o$ with temperature deviation from *ISA* conditions. Solid lines indicate numerical values, whilst dashed lines indicate the approximate solution. Solid symbols are for an (*m*/*MTOM*) of 1.0, whilst, for open symbols, (*m*/*MTOM*) = 0.8.

greatest sensitivity. By contrast, $(\eta_o L/D)_o$ decreases as temperature rises with a 20K increase reducing $(\eta_o L/D)_o$ by about 1%. The optimum Mach number is not shown in Fig. 10, since it has no significant dependency upon temperature. In all cases, the approximate solution is in excellent agreement with the numerical results.

4.4 Non-optimum conditions

In order to determine the cruise fuel burn under non-optimum conditions, the relations for the optimum conditions are combined with Equation (32) to give a single expression that enables $(\eta_o L/D)$ for an aircraft of fixed mass to be obtained for any combination of Mach number and altitude within the range of validity of the basic expressions.

In the constant Reynolds number case, i.e. from Equation (A-6) of Appendix A,

$$\frac{(\eta_o L/D)}{(\eta_o L/D)_o^R} \approx f_1 \left(1 + \frac{A}{2}\left(\left(\frac{1}{f_2}\frac{C_L}{(C_L)_o^R}\right) - 1\right)^2 + \frac{B}{6}\left(\left(\frac{1}{f_2}\frac{C_L}{(C_L)_o^R}\right) - 1\right)^3\right) \quad \ldots(112)$$

Here, f_1, f_2, A and B, as given in Appendix A, are all functions of ζ. These can be expressed in terms of M/M_o by recalling that, from Equations (21), (29) and (51)

$$\zeta = \frac{M}{\psi_4} = \frac{M}{M_o^R} = \frac{M}{M_o}(1+\varepsilon) \quad \ldots(113)$$

For an aircraft of fixed mass, if both the altitude and the speed are variable, then, from Equation (5),

$$\frac{C_L}{(C_L)_o} = \left(\frac{\chi}{\chi_o}\right)\left(\frac{M_o}{M}\right)^2 \quad \ldots(114)$$

Therefore, when the Reynolds number is allowed to vary, using the results from Equations (91) and (94),

$$\frac{(\eta_o L/D)}{(\eta_o L/D)_o} \approx f_1 \left(\frac{\left(C_F^{ac}\right)_o}{C_F^{ac}} \right)^{\left(\frac{1+\tau}{2}\right)} \left(1 + \frac{A}{2} \left(\left(\left(\frac{1+\Delta_o-\varepsilon}{f_2} \right) \left(\frac{\left(C_F^{ac}\right)_o}{C_F^{ac}} \right)^{\left(\frac{1-\tau}{2}\right)} \frac{C_L}{(C_L)_o} \right) - 1 \right)^2 \right.$$

$$\left. + \frac{B}{6} \left(\left(\left(\frac{1+\Delta_o-\varepsilon}{f_2} \right) \left(\frac{\left(C_F^{ac}\right)_o}{C_F^{ac}} \right)^{\left(\frac{1-\tau}{2}\right)} \frac{C_L}{(C_L)_o} \right) - 1 \right)^3 \right) \qquad \ldots (115)$$

From Equations (28) and (69),

$$\frac{\left(C_F^{ac}\right)_o}{C_F^{ac}} = \left(\left(\frac{1+1.34\overline{\Delta T}_o}{1+1.34\overline{\Delta T}} \right) \chi_o^{(i_o-i)} \left(\frac{M}{M_o} \right)^{(1-2i)} \right)^b \left(\frac{(C_L)_o}{C_L} \right)^{ib} \qquad \ldots (116)$$

Therefore, if

$$f_3 \approx f_1 \left(\frac{\left(C_F^{ac}\right)_o}{C_F^{ac}} \left(\frac{C_L}{(C_L)_o} \right)^{ib} \right)^{\left(\frac{1+\tau}{2}\right)} \qquad \ldots (117)$$

and

$$f_4 \approx \frac{(1+\Delta_o-\varepsilon)}{f_2} \left(\frac{\left(C_F^{ac}\right)_o}{C_F^{ac}} \left(\frac{C_L}{(C_L)_o} \right)^{ib} \right)^{\left(\frac{1-\tau}{2}\right)}, \qquad \ldots (118)$$

then

$$\frac{(\eta_o L/D)}{(\eta_o L/D)_o} \approx f_3 \left(\frac{(C_L)_o}{C_L} \right)^{ib\left(\frac{1+\tau}{2}\right)} \left(1 + \frac{A}{2} \left(\left(f_4 \left(\frac{C_L}{(C_L)_o} \right)^{\upsilon} \right) - 1 \right)^2 \right.$$

$$\left. + \frac{B}{6} \left(\left(f_4 \left(\frac{C_L}{(C_L)_o} \right)^{\upsilon} \right) - 1 \right)^3 \right), \qquad \ldots (119)$$

where

$$\upsilon = 1 - ib \left(\frac{1-\tau}{2} \right) \qquad \ldots (120)$$

Equation (119) is a completely general relation that can be used to estimate $(\eta_o L/D)$ for an aircraft of specified weight at any combination of speed and altitude, provided that the corresponding Mach numbers and lift coefficients fall within the range of validity of the expressions given in Appendix A. Whilst the extension to include Reynolds number has introduced greater complexity, the basic simplicity of the original relation, i.e. Equation (112), is

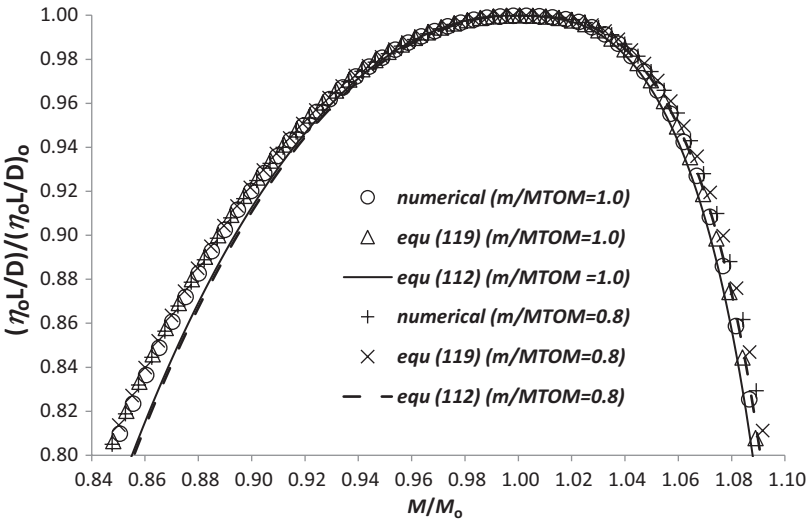

Figure 11. The variation of normalised ($\eta_o L/D$) with normalised Mach number in the *ISA* for two values of *m*/*MTOM* when χ is fixed at the optimum value, χ_o.

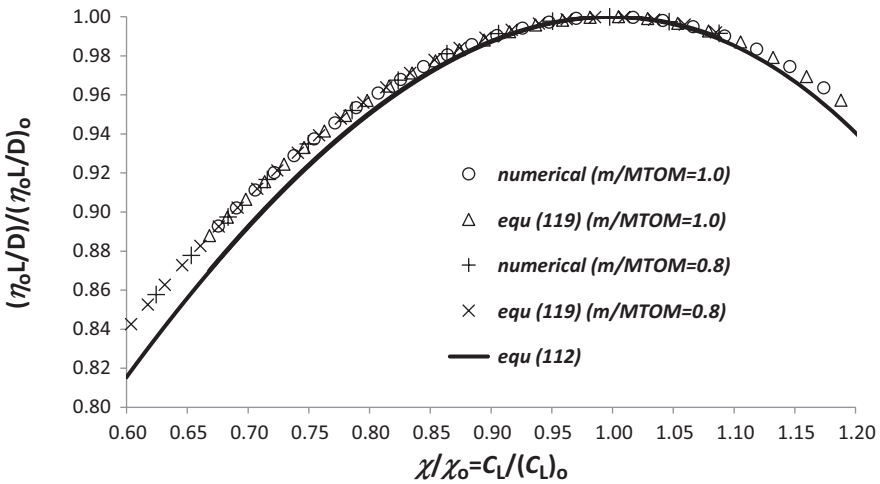

Figure 12. The variation of normalised ($\eta_o L/D$) with normalised lift coefficient in the *ISA* for two values of *m*/*MTOM* when *M* is equal to M_o.

preserved, with Equations (51), (91) and (94) providing the values of the three fundamental normalising quantities M_o, $(C_L)_o$ and $(\eta_o L/D)_o$ identified in Ref. 1.

In order to illustrate the effects of Reynolds number and to assess the accuracy of the approximations, estimates from Equation (119) are compared with numerical solutions of Equation (23), for the same example aircraft used for Figs. 7–10 flying in the ISA. These results are presented in Figs. 11 and 12. Figure 11 shows the effect of changing the Mach number relative to M_o, whilst the aircraft follows the isobar for optimum ($\eta_o L/D$). Results are shown for two values of the mass ratio. When *m*/*MTOM* is equal to one, the aircraft

is in the tropopause and in the stratosphere when it is 0.8. Results for constant Reynolds number, i.e. from Equation (112), are also shown. In this case, the influence of mass is very weak and the change in normalised $(\eta_o L/D)$ for a given Mach number change is reduced slightly relative to the constant Reynolds number case. Results from Equation (119) are in good agreement with the numerical solutions. Figure 12 shows the situation in which the Mach number is fixed at M_o and the aircraft is flying in the *ISA* along a range of isobars. Away from the optimum isobar, $(\eta_o L/D)$ is reduced. Once again, when Reynolds number is allowed to vary, the reduction is lower than for the constant Reynolds number case and the effect of variations in mass are small. There is seen to be excellent agreement between the approximate and numerical results. Therefore, the Reynolds number affects both the optimum values themselves and the variations relative to the optimum when speed and altitude are changed.

4.5 The effect of temperature profile

When Reynolds number effects are accounted for, the optimum flight level depends on the variation of atmospheric temperature with altitude. As indicated in Fig. 6, actual temperature profiles usually deviate from the International Standard Atmosphere and there are systematic profile changes with both latitude and season. For example, the tropopause occurs at about 10km in the northern latitudes, but nearer to 16km in the tropics. In addition, there are weather dependent temperature variations and changes in the tropopause height that may be relevant for flight optimisation. Locally, temperature deviations from *ISA* in excess of ±20K are not uncommon. Real temperature profiles can also have vertical temperature gradients that differ considerably from the *ISA*. Non-monotonic temperature changes, with large lapse rate variations occurring over just a few meters vertically, can occur anywhere at any altitude. Typically, vertical temperature changes stay above –0.3K/FL because for smaller values the atmosphere is unstably layered. However, large positive gradients are possible at inversion layers, with an important example being the tropopause inversion layer. Here there is a region, just above the tropopause, about 1km deep, with increasing temperature (Birner et al.[9]). Since temperature profiles are predictable, at least to some degree, the actual profile, or, at least, an average along the flight path, could be considered for optimised flight planning.

An example of the variation of the optimum *FL* with mass ratio for the example aircraft used in the previous sections operating in the two atmospheric conditions shown in Fig. 6 is given in Fig. 13. These results are obtained using Equation (100). For *ISA* conditions, there is only one optimum Flight Level for each value of the mass ratio. However, in the case of the example "real" atmosphere in Fig. 6, for some values of the mass ratio there are multiple solutions, e.g. between 0.86 and 0.88, there are five values of $(FL)_o$ for each mass ratio. However, as previously described, each Flight Level and mass ratio pair has a corresponding value of $(\eta_o L/D)_o$ and, in the case of multiple solutions at a particular mass ratio, one will have a value that is higher than the rest. These values are found from Equation (94) and selecting the points with the largest $(\eta_o L/D)_o$ at each value of the mass ratio allows the "optimum climb" profile to be determined. This is shown as the solid line in the figure and it is found to be in good agreement with the numerical results.

The corresponding values of the optimum Mach number are given in Fig. 14. These come from Equations (51) and (57). It is interesting to note that, in those parts of the atmosphere where the lapse rate is constant, M_o is almost constant, whilst $(FL)_o$ increases as the mass decreases. However, as previously noted, when the optimum flight level is independent of the mass, i.e. when there is a lapse rate discontinuity, the aircraft must adjust its speed

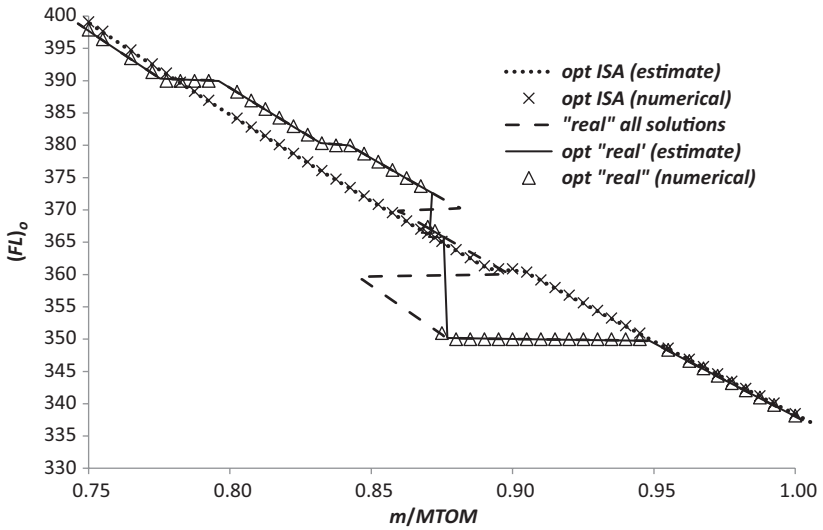

Figure 13. Optimum Flight Level as a function of aircraft mass for the atmospheric temperature profiles given in Fig. 6. The aircraft characteristics are the same as those used for Figs. 7–12.

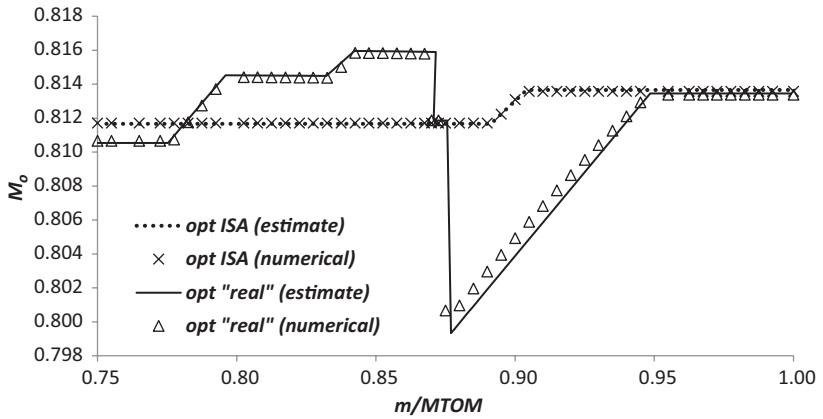

Figure 14. Optimum Mach number as a function of aircraft mass for the atmospheric temperature profiles given in Fig. 6.

progressively as the mass reduces. The numerical results suggest that the linear variation assumed in the approximate solution is reasonable. In this example, the maximum change required is about 2%.

Finally, the percentage difference between $(\eta_o L/D)_o$ in the example "real" atmosphere and the *ISA* for a given aircraft mass ratio is shown in Fig. 15. This is a very severe test of the accuracy of the approximate solution and, since there are discontinuities, the accuracy of the numerical method. However, the agreement between the two is good. In this example, the differences between the two atmospheric temperature profiles produce changes in $(\eta_o L/D)_o$ approaching 1%. Whilst this is small, in aircraft operations fuel use is managed to about 1%, making this variation significant and worthy of closer investigation.

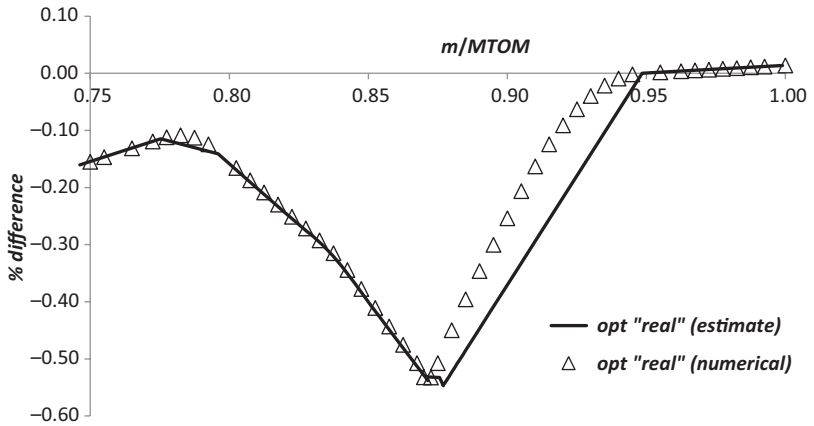

Figure 15. The percentage difference between $(\eta_o L/D)_o$ in the example "real" atmosphere in Fig. 6 and in the *ISA* as a function of the mass ratio.

5.0 CONCLUSION

A method that allows the estimation of $(\eta_o L/D)$ for a turbofan powered aircraft with a specified weight, operating over a wide range of altitude and Mach number in a general atmosphere, characterised by the variation of temperature with pressure, has been developed. It accounts fully for the corresponding variations in Reynolds number. The general problem is complex, and the governing equations can be solved with iterative numerical schemes. However, by using power-law approximations and establishing "order of magnitude" estimates for the various terms, simple, accurate and explicit relations have been developed for the key quantities, together with equations for the general variation of $(\eta_o L/D)$ with Mach number and lift coefficient. These approximate solutions are expressed as perturbations to those for flight in an atmosphere with a constant temperature of 216.65K, i.e. the ISA stratosphere. They are shown to be in good agreement with the corresponding numerical values over the range of conditions for which the basic, constant Reynolds number, model is known to be valid. Since the absolute accuracy depends upon the fidelity of the basic empirical relations, as new information becomes available, these may need to be modified, the analysis repeated, and the results updated. The ability to be developed and improved in this way is a key feature of the method.

It has been found that the Reynolds number for optimum $(\eta_o L/D)$ increases as the aircraft mass and the vertical temperature gradient increase, but decreases as the difference between the local static temperature and the *ISA* value increases. The corresponding lift coefficient, $(C_L)_o$, decreases as both aircraft mass and temperature gradient increase and increases when ΔT rises. Consequently, the optimum altitude increases as ΔT increases, but decreases as both the mass and the temperature gradient increase. The optimum Mach number decreases as the temperature gradient increases and increases as ΔT increases. Finally, $(\eta_o L/D)_o$ decreases as the mass decreases and ΔT increases, whilst increasing as the temperature gradient increases.

For flight in the *ISA*, when the speed and altitude differ from their values at the optimum, $(\eta_o L/D)$ is reduced. However, the reduction is less than that found in the constant Reynolds number case. The alleviation is not large, but it is significant.

The method has been used to determine the variation of Mach number and altitude for a minimum fuel use cruise when operating in a realistic atmosphere with a complex temperature variation with altitude. It is found that, when Reynolds number effects are included, the

optimum cruise-climb profile involves significant variations in both Mach number and lift coefficient.

For application to a given aircraft, five independent coefficients must be specified. These are all constants and fundamental characteristics of the airframe and engine combination. Whilst two of them are simple parameters involving aircraft weight and size, the remaining three are equivalent to the constant quantities $(\eta_o L/D)_o$, $(C_L)_o$ and M_o required in the original, constant Reynolds number, formulation. They are complex quantities that must be determined by either theoretical, or empirical, means. The estimation of the values of these parameters for a given aircraft will be considered in Part 2.

REFERENCES

1. POLL, D.I.A. On the relationship between non-optimum operations and fuel requirement for large civil transport aircraft with reference to environmental impact and contrail avoidance, *Aero J*, 2018, **122**, (1258), pp 1827–1870.
2. SHEVELL, R.S. *Fundamentals of Flight* (2nd ed), Prentice Hall, 1989, ISBN 0-13-339060-8.
3. ESDU Subsonic lift-dependent drag due to the trailing vortex wake for wings without camber of twist. Engineering Sciences Data Unit Item 74035, October 1974 (amended April 1996).
4. CUMPSTY, N.A. and HAYES, A.L. *Jet Propulsion* (3rd ed), Cambridge University Press, 2015, ISBN 978-107-51122-4.
5. VON KÁRMÁN, T. Turbulence and skin friction. *J Aero Sci*, 1934, **1**, pp 1–20.
6. VAN DRIE, E.R. Turbulent boundary layers in compressible flow. *J Aero Sci*, 1951, **18**, pp 145–160.
7. EASA, Airbus A318-A319-A320-A321 Type-Certificate Data Sheet, TCDS A.064 Issue 02, European Aviation Safety Agency, 2006.
8. ICAO, Manual of the ICAO Standard Atmosphere, Rep., ICAO Document No. 7488, 2nd Edition, 1964.
9. BIRNER, T., DÖRNBRACK, A. and SCHUMANN, U. How sharp is the tropopause at midlatitudes? *Geophys Res Lett*, 2002, **29**, (14), pp 45-1–45-4, doi: 10.1029/2002gl015142.

APPENDIX A. THE "UNIVERSAL" NORMALISING FUNCTIONS FOR THE CONSTANT REYNOLDS NUMBER CASE

In Ref. 1, it is shown that[8]

$$\frac{(\eta_o L/D)}{(\eta_o L/D)_o^R} = \frac{(\eta_o L/D)_B^R}{(\eta_o L/D)_o^R}\left(\frac{(\eta_o L/D)^R}{(\eta_o L/D)_B^R}\right) = Function\left(\frac{C_L}{(C_L)_o^R}, \frac{M_\infty}{M_o^R}\right), \qquad \ldots (A\text{-}1)$$

where subscript B (= best) refers to the maximum value of $(\eta_o L/D)$ at a given Mach number, whilst the subscript o refers to the optimum value. The first term on the right-hand side is a function of the ratio of the flight Mach number to the optimum Mach number only. In reality, this is a single, smooth and continuous function. However, for simplicity, in Ref. 1, it was

[8]In reference 1, subscript "ηLDm" is used to denote the condition at which $(\eta L/D)$ is a maximum for a given Mach number and subscript "opt" is used for the absolute maximum, or optimum, condition. To simplify the text in this paper, these subscripts have been changed to "B", for *best* and "o" for opt, respectively.

approximated by two separate relations, i.e. for $0.80 < M_\infty/M_o^R < 1.0$,

$$\frac{(\eta_o L/D)_B^R}{(\eta_o L/D)_o^R} = f_1 \approx 1 - 6.00\left(\frac{M_\infty}{M_o^R} - 1\right)^2 - 15.0\left(\frac{M_\infty}{M_o^R} - 1\right)^3, \quad \ldots (A\text{-}2)$$

whilst, for $1.0 \le M_\infty/M_o^R < 1.08$,

$$f_1 \approx 1 - 233\left(\frac{M_\infty}{M_o^R} - 1\right)^3 \quad \ldots (A\text{-}3)$$

Unfortunately, Equations (A-2) and (A-3) do not have the same curvature when M_∞ is equal to M_o^R. This is a consequence of the choice of the approximating functions. The discontinuity has no basis in physics and, when using the method to identify optima in regions where M_∞ is close to M_o^R, it may cause numerical problems. However, any potential difficulty can be eliminated by replacing Equations (A-2) and (A-3) with a function whose characteristics give a continuous and smooth curvature over the full parameter range. This revised model is

$$f_1 \approx 1 - 6.00\left(\frac{M_\infty}{M_o^R} - 1\right)^2 - 15.0\left(\frac{M_\infty}{M_o^R} - 1\right)^3, \quad \ldots (A\text{-}4)$$

for $0.80 < M_\infty/M_o^R < 0.99$ and

$$f_1 \approx 1 - 5.8965\left(\frac{M_\infty}{M_o^R} - 1\right)^2 + 0.36024\left(\frac{M_\infty}{M_o^R} - 1\right)^3 - 31.684\left(\frac{M_\infty}{M_o^R} - 1\right)^4 - 53313\left(\frac{M_\infty}{M_o^R} - 1\right)^5, \quad \ldots (A\text{-}5)$$

if $0.99 \le M_\infty/M_o^R < 1.08$.

As can be seen in Fig. A-1, this new version of f_1 is in good agreement with the original functions except at the higher Mach numbers where the agreement with the data is improved.

The second term on the right-hand side of (A-1) may be approximated by the function

$$\frac{(\eta_o L/D)}{(\eta_o L/D)_B^R} \approx 1 + \frac{A}{2}\left(\frac{C_L}{(C_L)_B^R} - 1\right)^2 + \frac{B}{6}\left(\frac{C_L}{(C_L)_B^R} - 1\right)^3, \quad \ldots (A\text{-}6)$$

where the coefficients A and B depend upon M_∞/M_o^R only. It is found that, for $(M_\infty/M_o^R) < 0.975$,

$$A = B \approx -2.6, \quad \ldots (A\text{-}7)$$

otherwise

$$A \approx -\left(2.6 + 120\left(\frac{M_\infty}{M_o^R} - 0.975\right)^2\right) \quad \ldots (A\text{-}8)$$

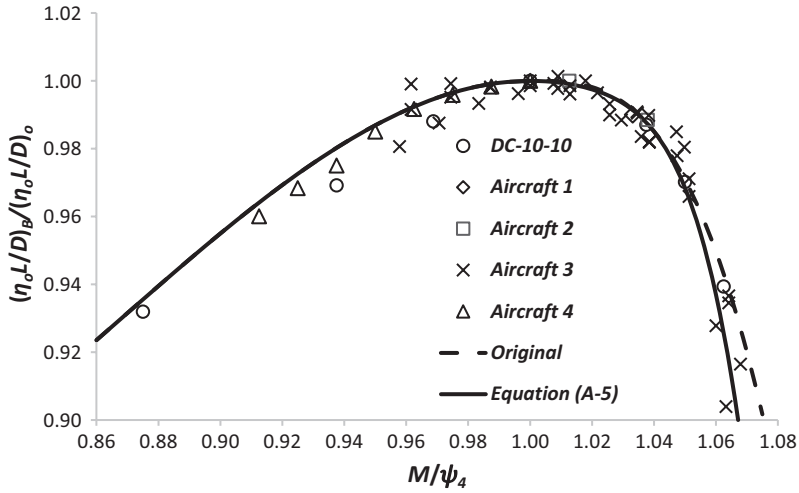

Figure A-1. The comparison between the new and the original approximations for the function f_1 – see Fig. 9 of Ref. 1.

and

$$B \approx -\left(2.6 + 270\left(\frac{M_\infty}{M_o^R} - 0.975\right)^2\right) \quad \ldots \text{(A-9)}$$

Finally,

$$\frac{C_L}{(C_L)_B^R} = \left(\frac{C_L}{(C_L)_o^R}\right) / \left(\frac{(C_L)_B^R}{(C_L)_o^R}\right), \quad \ldots \text{(A-10)}$$

In Ref. 1, for $0.80 < M_\infty/M_o^R < 1.08$, the second term on the right-hand side is represented by

$$f_2 = \frac{(C_L)_B^R}{(C_L)_o^R} \approx 1.05 + 5.0\left(\frac{M_\infty}{M_o^R} - 0.80\right)^3 - 55\left(\frac{M_\infty}{M_o^R} - 0.80\right)^4 \quad \ldots \text{(A-11)}$$

However, in this paper a revised version has been adopted for the same M_∞/M_o^R range. This is

$$f_2 \approx 1.05 - 14.80\left(\frac{M_\infty}{M_o^R} - 0.80\right)^3 + 116.75\left(\frac{M_\infty}{M_o^R} - 0.80\right)^4 - 370\left(\frac{M_\infty}{M_o^R} - 0.80\right)^5 \quad \ldots \text{(A-12)}$$

This new function, whilst being more complex, has the advantage of providing a significantly better fit to the data over the whole range, but particularly at the higher Mach numbers – see Fig. A-2.

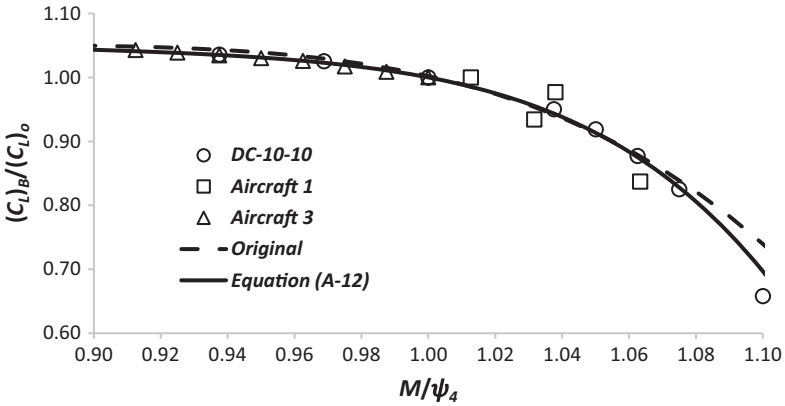

Figure A-2. The comparison between the new and the original approximations for the function f_2 – see Fig. 8 of Ref. 1.